Published in final edited form as:

Cell Rep. 2019 October 22; 29(4): 829–843.e5. doi:10.1016/j.celrep.2019.09.026.

RAG-Mediated DNA Breaks Attenuate PU.1 Activity in Early B Cells through Activation of a SPIC-BCLAF1 Complex

Deepti Soodgupta[1], **Lynn S. White**[1], **Wei Yang**[2], **Rachel Johnston**[1], **Jared M. Andrews**[3], **Masako Kohyama**[4], **Kenneth M. Murphy**[3], **Nima Mosammaparast**[3], **Jacqueline E. Payton**[3], **Jeffrey J. Bednarski**[1,5,*]

[1]Department of Pediatrics, Washington University School of Medicine, St. Louis, MO 63110, USA

[2]Department of Genetics, Washington University School of Medicine, St. Louis, MO 63110, USA

[3]Department of Pathology and Immunology, Washington University School of Medicine, St. Louis, MO 63110, USA

[4]Department of Immunochemistry, Research Institute for Microbial Diseases, Osaka University, Suita, Osaka 565-0871, Japan

[5]Lead Contact

SUMMARY

Early B cell development is regulated by stage-specific transcription factors. PU.1, an ETS-family transcription factor, is essential for coordination of early B cell maturation and immunoglobulin gene (*Ig*) rearrangement. Here we show that RAG DNA double-strand breaks (DSBs) generated during *Ig* light chain gene (*Igl*) rearrangement in pre-B cells induce global changes in PU.1 chromatin binding. RAG DSBs activate a SPIC/BCLAF1 transcription factor complex that displaces PU.1 throughout the genome and regulates broad transcriptional changes. SPIC recruits BCLAF1 to gene-regulatory elements that control expression of key B cell developmental genes. The SPIC/BCLAF1 complex suppresses expression of the SYK tyrosine kinase and enforces the transition from large to small pre-B cells. These studies reveal that RAG DSBs direct genome-wide changes in ETS transcription factor activity to promote early B cell development.

In Brief

ETS-family transcription factors are key regulators of early B cell development. Soodgupta et al. show that RAG-induced DNA breaks generated during antigen receptor gene recombination

*Correspondence: bednarski_j@wustl.edu.

AUTHOR CONTRIBUTIONS

D.S., L.S.W., W.Y., J.M.A., and R.J. performed experiments and data analyses. N.M. and J.E.P. provided expertise and assisted with data analyses. M.K. and K.M.M. provided mice and expertise for the studies. J.J.B. supervised the project, interpreted experiments, wrote the manuscript, and secured funding.

DECLARATION OF INTERESTS

The authors declare no competing interests.

SUPPLEMENTAL INFORMATION

Supplemental Information can be found online at https://doi.org/10.1016/j.celrep.2019.09.026.

activate a SPIC/BCLAF1 transcription factor complex that counters PU.1 activity and regulates gene expression changes to promote transition from large to small pre-B cells.

Graphical Abstract

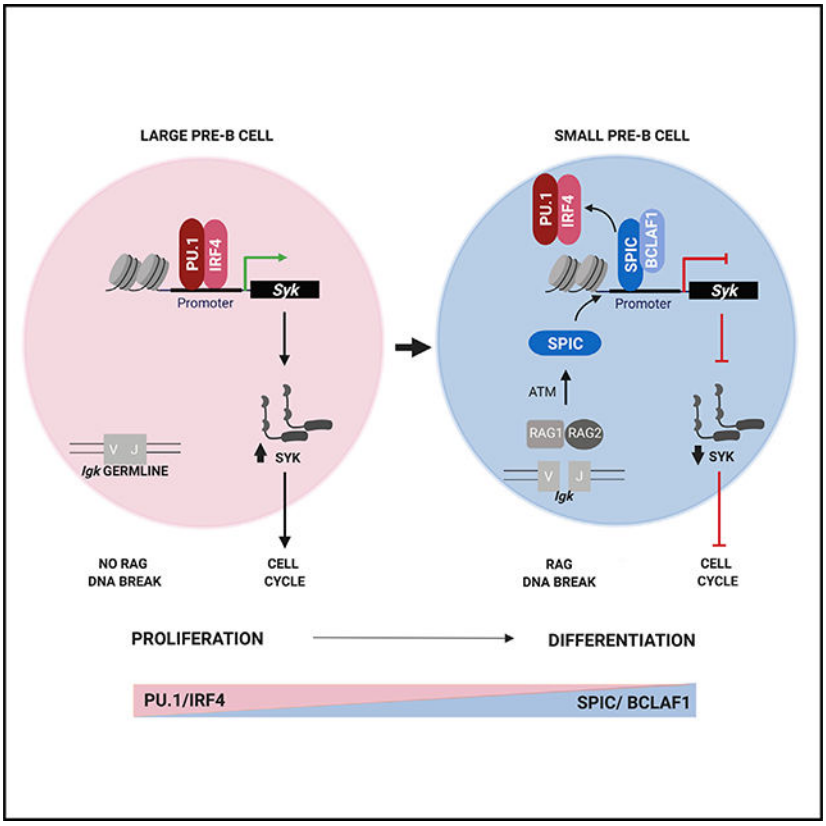

INTRODUCTION

B cell development requires the sequential assembly and expression of genes encoding the immunoglobin heavy (Igh) and immunoglobulin light (Igl) chains to generate a mature B cell receptor (BCR) (Rajewsky, 1996). *Ig* genes are assembled through the process of V(D)J recombination, which joins distant variable (V), joining (J), and diversity (D) segments (Fugmann et al., 2000). The DNA double-strand breaks (DSBs) necessary for V(D)J recombination are generated by the RAG endonuclease, which is composed of the RAG1 and RAG2 proteins (Fugmann et al., 2000). RAG-mediated DNA breaks are generated in the G1 phase of the cell cycle and activate the DNA damage response (DDR) kinase ATM, which facilitates repair of the broken DNA ends through nonhomologous end joining (Helmink and Sleckman, 2012). In response to RAG DSBs, ATM also activates a broad transcriptional program that regulates genes involved in diverse B cell functions, including migration, cell-cycle arrest, survival, and differentiation (Bednarski et al., 2012, 2016; Bredemeyer et al., 2008; Helmink and Sleckman, 2012; Steinel et al., 2013). This genetic program is mediated by ATM-dependent activation of several transcription factors, including NF-κB1, NF-κB2, and SPIC (Bednarski et al., 2012, 2016; Bredemeyer et al., 2008).

The *Igh* gene is assembled first in pro-B cells and productive rearrangement results in its surface expression with surrogate light chains (λ5 and VpreB) to generate the pre-BCR, which signals transition to the large pre-B cell stage (Clark et al., 2014; Herzog et al., 2009; Rajewsky, 1996). Pre-BCR oligomerization signals through the SYK tyrosine kinase to promote proliferation and clonal expansion of large pre-B cells (Clark et al., 2014; Herzog et al., 2009). Activation of SYK also triggers *Igl*κ (*Igk*) gene recombination (Clark et al., 2014). RAG expression is suppressed in proliferating cells, and as such, *Igk* gene assembly requires induction of cell-cycle arrest and transition to the small, non-proliferating pre-B cell stage (Clark et al., 2014; Desiderio et al., 1996; Johnson et al., 2008; Ochiai et al., 2012). RAG DSBs activate ATM-dependent DDR signaling pathways that enforce cell-cycle arrest and promote survival to prevent proliferation of cells with unrepaired DSBs and permit time for proper assembly of *Igk* genes (Bednarski et al., 2012, 2016; DeMicco et al., 2016).

B cell development and assembly of *Ig* genes are carefully orchestrated by developmental stage-specific transcription factors, including E2A, EBF, Pax5, PU.1 and SPIB (Pang et al., 2014). The ETS-family transcription factor PU.1 is required for B cell lineage commitment and is constitutively expressed throughout B cell development (Polli et al., 2005; Schweitzer and DeKoter, 2004; Scott et al., 1994, 1997). PU.1 has critical functions during B cell maturation. In pre-B cells, PU.1 regulates expression of a diverse genetic program, including genes involved in B cell proliferation, differentiation, and *Ig* gene rearrangement (Batista et al., 2017; Heinz et al., 2010; Solomon et al., 2015). Expression of SYK and germline transcription of *Igk,* which are required for pre-BCR signaling and initiating V(D) J recombination, respectively, depend on PU.1 activity (Batista et al., 2017; Herzog et al., 2009; Schwarzenbach et al., 1995; Schweitzer and DeKoter, 2004). Interestingly, loss of PU.1 in B cell progenitors results in only a mild defect in B cell development because of compensatory function of another ETS-family transcription factor, SPIB (Polli et al., 2005; Sokalski et al., 2011; Ye et al., 2005). PU.1 and SPIB associate with nearly identical regions of the genome in B cells and regulate transcription of a similar cohort of genes (Solomon et al., 2015). Combined loss of PU.1 and SPIB impairs B cell maturation in the bone marrow and predisposes to the development of B cell leukemia (Sokalski etal., 2011).

We previously demonstrated that SPIC, an ETS-family transcriptional repressor with homology to PU.1 and SPIB, also functions in pre-B cells (Bednarski et al., 2016; Bemark et al., 1999; Hashimoto et al., 1999). Unlike PU.1 and SPIB, SPIC is not constitutively expressed in early B cells but, rather, is induced by signals from RAG DSBs (Bednarski et al., 2016). SPIC operates primarily as a transcriptional repressor and counters the activating functions of PU.1 and SPIB (Li et al., 2015; Zhu et al., 2008). In pre-B cells, SPIC suppresses expression of *Syk* and *Blnk,* which inhibits pre-BCR signaling and enforces cell-cycle arrest in pre-B cells with RAG DSBs (Bednarski et al., 2016). SPIC also inhibits transcription of *Igk* to prevent generation of additional RAG DSBs (Bednarski et al., 2016). Binding of SPIC to gene-regulatory elements for *Syk, Blnk,* and *Igk* is associated with loss of PU.1 at these genomic regions. Thus, expression of SPIC antagonizes PU.1 as these identified genes to suppress transcription and coordinate pre-B cell development.

Whether SPIC has broader functions in gene regulation and its mechanism of action in B cells have not been defined. SPIC may oppose PU.1 at limited gene targets or, alternatively,

may modulate PU.1 activity throughout the genome. In this regard, attenuation of PU.1 activity by SPIC could suppress pre-B cell genetic programs to promote continued B cell maturation. SPIC may function simply by displacing PU.1 through competition for DNA binding sites or may complex with other transcriptional regulators to repress transcription. We show here that, in response to RAG DSBs, SPIC binds throughout the genome of pre-B cells and elicits global changes in PU.1 chromatin association. SPIC associates with the transcriptional repressor BCLAF1 (Bcl2-associated factor 1) to regulate a distinct subset of RAG DSB-dependent gene expression changes and to enforce transition from large to small pre-B cells. These experiments provide insight into the regulation of ETS transcription factors in early B cells and the impact of DDR signaling on B cell development.

RESULTS

RAG DSB Signals Induce Genome-Wide Changes in PU.1 Binding

To determine the effects of DNA damage signaling on PU.1 activity in early B cells, we used Abelson-kinase transformed pre-B cells (abl pre-B cells) deficient in RAG1 or the Artemis endonuclease that express the *Bcl2* transgene (*Rag1*$^{-/-}$*:Bcl2* and *Art*$^{-/-}$*:Bcl2,* respectively) (Bredemeyer et al., 2008). Expression of the Abl kinase promotes pre-B cell proliferation and suppresses expression of *Rag1* and *Rag2.* Treatment with the Abl kinase inhibitor imatinib triggers cell-cycle arrest, induction of RAG expression, and recombination of *Igk* (Bredemeyer et al., 2008). The *Bcl2* transgene supports survival of imatinib-treated cells. Following treatment with imatinib, *Rag1*$^{-/-}$*:Bcl2* abl pre-B cells do not generate RAG DSBs. In contrast, *Art*$^{-/-}$*:Bcl2* abl pre-B cells generate RAG DSBs at *Igk*, but these DSBs are not repaired as Artemis is required to open hairpin-sealed coding DNA ends (Figure 1A) (Bredemeyer et al., 2008; Helmink and Sleckman, 2012). The RAG DSBs in *Art*$^{-/-}$*:Bcl2* abl pre-B cells activate ATM-dependent DDRs (Bednarski et al., 2012, 2016; Bredemeyer et al., 2008).

Chromatin immunoprecipitation followed by next-generation DNA sequencing (ChIP-seq) reveals global changes in PU.1 binding in pre-B cells with RAG DSBs (*Art*$^{-/-}$*:Bcl2*) compared with pre-B cells without RAG DSBs (*Rag1*$^{-/-}$*:Bcl2*), despite no differences in PU.1 expression (Figures 1B, 1C, and S1A). Induction of RAG DSBs results in gain of few new binding sites but loss of approximately 20% of the PU.1 binding sites identified in *Rag1*$^{-/-}$*:Bcl2* abl pre-B cells (Figure 1B). Gene Ontology analysis demonstrates that genes within 12 kb of lost PU.1 binding sites are involved in immune cell activation and differentiation (Figure S1B). In contrast, PU.1 binding sites that are conserved between *Rag1*$^{-/-}$*:Bcl2* and *Art*$^{-/-}$*:Bcl2* abl pre-B cells are proximal to genes involved in cell homeostasis and maintenance (i.e., signaling, nuclear transport, apoptosis). Novel RAG DSB-induced PU.1 binding occurred near genes involved in cell adhesion and developmental processes. Induction of RAG DSBs did not alter PU.1 binding across genomic regulatory elements as equal binding to promoters, genes, or intergenic regions (i.e., enhancers) is observed in both *Rag1*$^{-/-}$*:Bcl2* and *Art*$^{-/-}$*:Bcl2* abl pre-B cells (Figure S1C). Thus, in response to RAG DSBs, pre-B cells have a genome-wide reduction in PU.1 chromatin binding, which is expected to result in changes in gene expression that affect important cellular functions.

Expression of SPIC Alters PU.1 Binding in Pre-B Cells

RAG DSBs trigger ATM-dependent induction of SPIC (Figure 2A). Expression of SPIC, in turn, results in loss of PU.1 binding at genes required for pre-BCR signaling (Bednarski et al., 2016). To determine if expression of SPIC is responsible for the global changes in PU.1 binding observed in response to RAG DSBs, we stably transduced *Rag1*$^{-/-}$*:Bcl2* abl pre-B cells with a lentiviral vector encoding a tetracycline-inducible FLAG-HA-tagged SPIC (*Rag1*$^{-/-}$*:Bcl2:Spic*^{tet}). Treatment with doxycycline induced equivalent SPIC mRNA expression as triggered by RAG DSBs (Figures 2A and 2B). We performed ChIP-seq for PU.1 in *Rag1*$^{-/-}$*:Bcl2:Spic*^{tet} abl pre-B cells treated with imatinib alone or in combination with doxycycline to induce expression of SPIC (Figure 2B). Expression of SPIC does not alter PU.1 expression but results in significant changes in PU.1 chromatin binding (Figures 2C and 2D). Moreover, expression of SPIC results in changes in PU.1 binding that are similar to changes induced by RAG DSBs (compare Figures 1B and 2D). These findings demonstrate that changes in PU.1 binding in response to RAG DSBs are, in large part, due to RAG DSB-mediated induction of SPIC.

SPIC and PU.1 Bind to Identical Genomic Regions

SPIC and PU.1 have homologous DNA binding domains and have been previously shown *in vitro* to bind to the same DNA sequence (Bemark et al., 1999; Hashimoto et al., 1999). Current commercial antibodies against endogenous SPIC do not work for ChIP. Thus, to determine if SPIC and PU.1 binding to chromatin is similarly distributed throughout the genome, we performed ChIP-seq with anti-HA antibodies to precipitate FLAG-HA-SPIC in *Rag1*$^{-/-}$*:Bcl2:Spic*^{tet} abl pre-B cells treated with doxycycline (to induce SPIC). Results were compared with findings from ChIP-seq for PU.1 in *Rag1*$^{-/-}$*:Bcl2* abl pre-B cells without SPIC expression. Peaks with ≥1 bp of overlap between the two ChIP-seq datasets were considered as enriched for binding to both transcription factors. We find that SPIC and PU.1 bind to similar locations throughout the genome (Figure 3A). Additionally, PU.1 binding is lost at sites where SPIC is bound (Figures 3B, 3C, and S2).

The ChIP peaks for SPIC and PU.1 in regions where both transcription factors bind (common peaks in Figure 3A) have significant nucleotide overlap (Figures 3D). Indeed, the majority of these shared binding sites overlap by >70%, and the greatest number of ChIP peaks have >90% overlap. Furthermore, SPIC and PU.1 bind to similar regions throughout the genome (Figure 3E). Collectively, these findings demonstrate that SPIC and PU.1 bind to similar regulatory elements in pre-B cells and that SPIC binding results in displacement of PU.1 from these regions.

SPIC Recruits BCLAF1 to Chromatin

PU.1 forms heterodimeric complexes with IRF4 or IRF8 to regulate transcription initiation (Brass et al., 1996; Heinz et al., 2010). SPIC does not complex with IRF4 or IRF8 but binds to similar DNA sequences as PU.1 (Carlsson et al., 2003). These findings raise the question of whether SPIC complexes with distinct protein partners to regulate gene expression. To identify SPIC interacting partners, we generated *Arf*$^{-/-}$*:Bcl2* abl pre-B cells expressing either a tetracycline-inducible FLAG-HA-tagged SPIC (*Arf*$^{-/-}$*:Bcl2:Spic*^{tet}) or a tetracycline-inducible FLAG-HA-tagged PU.1 (*Arf*$^{-/-}$*:Bcl2:Pu1*^{tet}). Cells were treated with

imatinib to induce RAG DSBs and with doxycycline to induce comparable expression of the FLAG-tagged transcription factors (Figure S3). SPIC and PU.1 were immunoprecipitated using anti-FLAG antibodies, and associated proteins were identified by tandem mass spectrometry. Unique peptides were compared with identify proteins enriched for binding to SPIC (Figure 4A; Table S1). We focused on nuclear proteins with functions in transcriptional regulation. One of these proteins that enriched for binding to SPIC and not PU.1 is BCLAF1 (Figures 4A and 4B). BCLAF1 was originally identified as a transcriptional repressor but has also been shown to promote gene expression in response to DNA damage (Kasof et al., 1999; Liu et al., 2007; Shao et al., 2016). *Bclaf1*-deficient mice have reduced T cells and increased splenic B cell numbers, suggesting that BCLAF1 may function in immune development (McPherson et al., 2009).

Reciprocal co-immunoprecipitation experiments demonstrate that BCLAF1 selectively associates with SPIC and not PU.1 in $Art^{-/-}$*:Bcl2* abl pre-B cells (Figures 4B and 4C). In contrast, IRF4 and IRF8 associate with PU.1 but do not complex with SPIC (Figure 4B). To determine if BCLAF1 is recruited to SPIC-bound chromatin in pre-B cells, we compared BCLAF1 ChIP-seq with SPIC ChIP-seq. A significant portion (>80%) of BCLAF1 and SPIC peaks overlap indicating that the two proteins associate with similar chromatin regions (Figure 4D). Consistent with ChIP-seq results, BCLAF1 binding to the *Syk* promoter is increased in cells expressing SPIC (Figure 4E). Additionally, ChIP-re-ChIP experiments show that BCLAF1 only associates with the SPIC-bound *Syk* promoter and not with the PU.1-bound promoter (Figure 4F). Finally, BCLAF1 binding to the *Syk* promoter is increased in pre-B cells with RAG DSBs ($Art^{-/-}$*:Bcl2*), which express SPIC (Figures 4G and 2A). BCLAF1 ChIP peaks contain the conserved ETS DNA binding sequence (GGAA, $p < 1 \times e^{-33}$) suggesting that it may not directly bind DNA but rather is recruited to chromatin by SPIC in response to RAG DSBs in pre-B cells.

SPIC and BCLAF1 Regulate Gene Expression in Pre-B Cells

We previously showed that in response to RAG DSBs, SPIC represses expression of key genes required for pre-BCR signaling (Bednarski et al., 2016). Given our current findings that SPIC and its partner BCLAF1 bind throughout the genome, we hypothesized that this complex regulates a broad genetic program in pre-B cells. To identify the genes regulated by SPIC, we compared transcriptional changes in $Rag1^{-/-}$*:Bcl2:*$Spic^{tet}$ abl pre-B cells with and without expression of SPIC. Expression of 866 genes was changed ≥ 2-fold (adjusted $p < 0.05$) following expression of SPIC (Figures 5A and S4A; Table S2). Knockdown of BCLAF1 in SPIC-expressing $Rag1^{-/-}$*:Bcl2:*$Spic^{tet}$ abl pre-B cells changes expression of 55% of SPIC-regulated genes (≥ 2-fold change, adjusted $p < 0.05$) (Figures 5B, 5C, and S4A; Table S2). Notably, genes repressed by SPIC were rescued following knockdown of BCLAF1 (Figures 5C and S4A). Gene Ontology analysis revealed that SPIC- and BCLAF1-dependent genes are enriched for immune processes in B cells (Figure S4B). Importantly, loss of BCLAF1 does not alter SPIC binding to the *Syk* promoter, suggesting that recruitment of BCLAF1 is needed for SPIC-mediated transcriptional changes but not for SPIC binding to chromatin (Figure 5D).

We then determined the contribution of SPIC/BCLAF to the genetic program regulated by RAG DSBs in pre-B cells. Gene profiling revealed that BCLAF1 regulates a significant portion of RAG DSB-mediated genes (540 of 717 genes, ≥2-fold change, adjusted $p < 0.05$; Figure 5E; Table S3). Comparison of RAG DSB-dependent (*Art*$^{-/-}$*:Bcl2* versus *Rag1*$^{-/-}$*:Bcl2;* Figure 5E), SPIC-dependent (*Rag1*$^{-/-}$*:Bcl2:Spic*^{tet} expressing SPIC versus *Rag1*$^{-/-}$*:Bcl2;* Figure 5A), and BCLAF1-dependent (*Art*$^{-/-}$*:Bcl2* expressing shBCLAF1 versus *Art*$^{-/-}$*:Bcl2;* Figure 5E) gene expression changes identified 141 genes whose expression is modulated by all three variables (Figures 5F, 5G, and S5A; Table S4). Approximately 25% of these genes have concordant changes in expression (repressed by RAG DSBs, repressed by SPIC, and rescued by loss of BCLAF1; Figure S5A). Pathway analyses are enriched for diverse B cell functions, including proliferation, cell adhesion, and cell death (Figure S5B). These findings demonstrate that the SPIC/BCLAF1 complex regulates a distinct genetic program in pre-B cells with RAG DSBs.

BCLAF1 Regulates Pre-BCR Signaling in Primary Pre-B Cells

To determine if BCLAF1 is required for regulation of SPIC function in primary pre-B cells, we expanded pre-B cells from *Rag1*$^{-/-}$*:µIgh:Bcl2* and *Art*$^{-/-}$*:µIgh:Bcl2* mice in the presence of interleukin-7 (IL-7) (Bednarski et al., 2012, 2016). The *µIgh* transgene permits expression of a pre-BCR, which promotes transition to the pre-B cell developmental stage (Bednarski et al., 2012, 2016). IL-7 promotes proliferation and expansion of large pre-B cells. Withdrawal of IL-7 induces cell-cycle arrest, transition to small pre-B cells, expression of RAG, and induction of RAG DSBs at *Igk* (Bednarski et al., 2012, 2016; Johnson et al., 2008; Ochiai et al., 2012; Rolink et al., 1991; Steinel et al., 2013). Consistent with our previous findings, withdrawal of IL-7 results in induction of SPIC and suppression of *Syk* transcripts in pre-B cells with RAG DSBs *(Art*$^{-/-}$*:µIgh:Bcl2)* (Figures 6A and 6B) (Bednarski et al., 2016). Loss of BCLAF1 does not alter induction of *Spic* but does lead to increased expression of *Syk* in *Art*$^{-/-}$*:µIgh:Bcl2* small pre-B cells (Figures 6A and 6B). Consistent with the rescue of *Syk* mRNA levels, SYK protein is increased in *Art*$^{-/-}$*:Igh:Bcl2* pre-B cells lacking BCLAF1 to levels equivalent to those observed in *Rag1*$^{-/-}$*:µIgh:Bcl2* pre-B cells (Figure 6C). On the basis of these results, we conclude that BCLAF1 is necessary for repression of SYK in response to RAG DSBs in primary small pre-B cells.

To assess BCLAF1 binding to the *Syk* promoter during wild-type pre-B cell development *in vivo,* we used *Spic*$^{igfp/igfp}$ mice, which contain an IRES-EGFP targeted to the 3′ non-coding exon of *Spic* (Haldar et al., 2014). Approximately 2% of small pre-B cells from *Spic*$^{igfp/igfp}$ mice are EGFP positive, indicative of SPIC expression (Figures 6D and 6E). EGFP-expressing small pre-B cells are not observed in *Atm*$^{-/-}$*:Spic*$^{igfp/igfp}$, indicating that induction of SPIC (and EGFP) depends on DNA damage signaling (Figure 6E). SPIC-expressing *Spic*$^{igfp/igfp}$ small pre-B cells (EGFP positive) have reduced PU.1 binding and increased BCLAF1 binding to the *Syk* promoter as well as decreased *Syk* expression (Figures 6F–6H) (Bednarski et al., 2016). These results suggest that SPIC/BCLAF1 complex is induced by DNA damage signals from transient RAG DSBs generated during *Igl* rearrangement in wild-type small pre-B cells.

Loss of BCLAF1 Alters Large to Small Pre-B Cell Transition

Activation of SYK downstream of the pre-BCR can promote pre-B cell proliferation in the absence of IL-7 signaling (Clark et al., 2014; Herzog et al., 2009; Ochiai et al., 2012; Rolink et al., 2000; Wossning et al., 2006). Given that loss of BCLAF1 prevents SPIC-mediated repression of SYK, we hypothesized that loss of BCLAF1 may alter pre-B cell proliferation and the transition from large to small pre-B cells during early B cell development. To test this, we generated *Bclaf1*$^{f/f}$*:Mb1-cre* mice, which have selective loss of BCLAF1 in B cells (Figure 7A) (Hobeika et al., 2006). Pre-B cells from *Bclaf1*$^{f/f}$*:Mb1-cre* and *Bclaf1*$^{f/f}$ mice were expanded in the presence of IL-7. Following IL-7 withdrawal, *Bclaf1*-deficient pre-B cells from *Bclaf1*$^{f/f}$*:Mb1-cre* mice have increased S-phase progression and increased *Syk* expression compared with pre-B cells from *Bclaf1*™ and *Mb1-cre* mice (Figures 7B–7D). These findings support a role for BCLAF1 in the regulation of pre-B cell proliferation possibly through modulation of SYK activity downstream of pre-BCR signaling.

We next assessed B cell populations *in vivo.* In our breeding, *Mb1-cre* mice have normal numbers of pro-B cells but reduced pre-B cells relative to littermate wild-type *Bclaf1*$^{f/f}$ mice (Figures 7E and S6). In contrast, *Bclaf1*$^{f/f}$*:Mb1-cre* mice have increased numbers of pre-B cells compared with *Mb1-cre* mice and are similar to *Bclaf1*$^{f/f}$ mice (Figure 7E). Interestingly, the increase in pre-B cells in *Bclaf1*$^{f/f}$*:Mb1-cre* mice is due primarily to larger numbers of large pre-B cells (Figure 7E). Loss of *Bclaf1* does not alter numbers of pro-B cells or small pre-B cells. Consistent with findings in cultured cells, *in vivo* large, proliferating pre-B cells from *Bclaf1*$^{f/f}$*:Mb1-cre* mice have increased *Syk* mRNA levels (Figure 7F). *Syk* expression is not altered in small pre-B cells (Figure 7F). We propose that BCLAF1 functions in response to RAG DSBs in pre-B cells to suppress *Syk* and enforce transition from the large to small pre-B cell developmental stage.

DISCUSSION

Here we show that RAG DSBs induce genome-wide changes in PU.1 localization and function, which coordinates a distinct genetic program in B cells undergoing *Ig* gene rearrangement. This modulation of PU.1 activity is mediated by RAG DSB activation of a SPIC/BCLAF1 transcriptional repressor complex. SPIC displaces PU.1 at gene regulatory sites but requires association with BCLAF1 to suppress transcription. This antagonistic function of SPIC/BCLAF1 coordinates a broad genetic program and enforces transition from large to small pre-B cells in response to RAG DSBs.

PU.1 is a key regulator of cell fate decisions during early hematopoiesis and is essential for generating B cells from hematopoietic progenitors (Dakic et al., 2007; DeKoter et al., 2002; Pang et al., 2018; Scott et al., 1994, 1997). PU.1 expression is high in myeloid cells, in which it is required to promote lineage specific gene expression (Heinz et al., 2010). In contrast, PU.1 expression is reduced during B cell differentiation and remains low in established B cells (Back et al., 2005; Nutt et al., 2005). This differential activity of PU.1 is critical for directing appropriate lineage commitment. Dysregulation of PU.1 expression leads to aberrant differentiation and can result in leukemic transformation (Anderson et al., 2002; Pang et al., 2016; Rosenbauer et al., 2004, 2006; Sokalski et al., 2011). PU.1 activity is also regulated through interaction with other transcription factors, which modulate its

DNA binding properties or its transcriptional function (Maitra and Atchison, 2000; Nerlov et al., 2000; Rogers et al., 2016). For example, in early lymphoid precursors, E2A association with PU.1 inhibits PU.1-induced transcription of myeloid genes and promotes B lymphoid differentiation (Rogers et al., 2016). We find that PU.1 activity is regulated at the pre-B cell developmental stage through RAG DSB-mediated induction of SPIC, which binds chromatin and displaces PU.1. This transcription factor exchange results in changes in expression of genes involved in pre-BCR signaling, B cell proliferation, and B cell differentiation.

SPIC and PU.1 have homologous DNA binding domains (Bemark et al., 1999; Hashimoto et al., 1999). As such, SPIC can compete for DNA binding sites occupied by PU.1, and binding of SPIC results in displacement of PU.1 from these sites. Interestingly, SPIC associates with >90% of the PU.1 sites, but PU.1 binding is lost at only approximately 20% of the regions it binds in the absence of SPIC expression (Figures 2D and 3A). It is conceivable, then, that SPIC and PU.1 may simultaneously bind specific regions of the genome, and SPIC binding may not always fully displace PU.1. Rather, binding of SPIC nearby PU.1 may alter PU.1 transcriptional activity or other transcriptional machinery at these sites. Alternatively, in an individual cell, each ETS site may be occupied by either SPIC or PU.1, but ChIP analysis on a bulk population is not sensitive enough to discriminate between these two different states.

In early B cells, PU.1 and SPIB are constitutively expressed and have complementary functions (Schweitzer and DeKoter, 2004; Scott et al., 1994, 1997; Sokalski et al., 2011; Solomon et al., 2015). As such, conditional deletion of either PU.1 or SPIB alone mildly alters B cell development, but loss of both transcription factors results in a block in B cell differentiation at the pro-B cell stage (Polli et al., 2005; Sokalski et al., 2011; Su et al., 1997; Ye et al., 2005). PU.1 and SPIB bind to similar regions throughout the genome of pro-B cells and regulate expression of key developmental genes, including *Syk* and *Blnk,* which are necessary for pre-BCR signaling and induction of proliferation of large pre-B cells (Solomon et al., 2015). We find that SPIC also binds to the same genomic sites as PU.1. Given that SPIB and PU.1 bind identical regions and have complementary functions in early B cells, SPIC is also expected to counter SPIB similar to our observed results for PU.1. In contrast to PU.1 and SPIB, SPIC is inducibly expressed in pre-B cells in response to RAG DSBs and functions primarily as a transcriptional repressor. Expression of SPIC opposes PU.1 and SPIB activity resulting in suppression of pre-BCR and BCR signaling in early B cells and mature B cells, respectively, leading to a block in B cell maturation or function (Bednarski et al., 2016; Zhu et al., 2008). Importantly, complete or permanent inhibition of PU.1 and SPIB could be detrimental to B cell development, as combined loss of these transcription factors results in leukemic transformation (Sokalski et al., 2011). In this regard, induced expression of SPIC by RAG DSBs permits for stage-specific and transient inhibition of PU.1 (and SPIB). SPIC expression is expected to be lost after RAG DSBs are repaired and associated DDR signaling is terminated. The reduction in SPIC would allow PU.1 (and SPIB) to rebind to chromatin and resume transcriptional activities necessary for mature B cell function. Thus, RAG DSBs regulate a temporary suppression of PU.1 to promote transition from large to small pre-B cells and then permit continued transition to antibody-producing mature B cells.

PU.1 forms heterodimeric complexes with IRF4 or IRF8 to promote transcription (Brass et al., 1996; Heinz et al., 2010; Pongubala et al., 1992). As such, combined loss of IRF4 and IRF8 results in similar abnormalities in B cell development as loss of PU.1 (Lu et al., 2003; Ma et al., 2006). SPIC binds the same DNA sequence as PU.1 but has a distinct protein-interaction domain and does not bind IRF4 or IRF8 (Carlsson et al., 2003). Thus, SPIC could mediate suppression of transcription simply through displacement of PU.1 and loss of associated transcription activation machinery (i.e., IRF4). Displacement of the PU.1/IRF4 complex alone, though, may be insufficient to repress transcription as this is not expected to result in rapid changes in histone modifications or RNA polymerase activity, which drive gene expression. Alternatively, in a manner similar to PU.1, SPIC may effect transcriptional inhibition by recruiting additional proteins to gene-regulatory elements. In this regard, we find that SPIC, but not PU.1, binds BCLAF1. BCLAF1 is not necessary for SPIC binding to chromatin but is required for transcriptional repression. On the basis of these findings, we propose that antagonism of PU.1 activity is mediated by a SPIC-BCLAF1 complex that binds to chromatin and suppresses key PU.1-regulated genes. Further studies are needed to determine the mechanism by which the SPIC-BCLAF1 complex regulates transcription (i.e., activity on histone epigenetics, RNA polymerase activity, and locus accessibility).

BCLAF1 was first identified as a transcriptional repressor but also functions as an activator to promote expression of p53 and cytokines in response to DNA damage (Kasof et al., 1999; Liu et al., 2007; Shao et al., 2016). BCLAF1 also has been identified as a component of the RNA splicing complex (Savage et al., 2014; Vohhodina et al., 2017). We find that in early B cells, BCLAF1 complexes with SPIC to repress gene expression in response to RAG-mediated DSBs. BCLAF1 chromatin binding nearly completely overlaps with SPIC-bound genomic regions. SPIC and BCLAF1 could bind DNA independently and then cooperatively suppress transcription. In this regard, *in vitro* studies have shown that BCLAF1 binds the interferon-stimulated response element (ISRE) (Qin et al., 2019). The sequence for binding of the PU.1/IRF4 heterodimer contains a portion of the ISRE site in series with an ETS motif. BCLAF1 and SPIC could bind this same sequence, or, alternatively, BCLAF1 may be recruited to gene regulatory regions through protein-protein interactions with SPIC, which binds ETS DNA sequences. The domains that govern SPIC and BCLAF1 protein interactions and DNA binding are currently being investigated.

We find that loss of BCLAF1 prevents RAG DSB- and SPIC-mediated repression of *Syk* mRNA expression. SYK is a key signaling molecule downstream of the pre-BCR and is required for the pre-BCR to promote proliferation of large pre-B cells (Clark et al., 2014; Herzog et al., 2009). We previously showed that in response to RAG DSBs, induction of SPIC suppresses pre-BCR signaling to enforce cell-cycle arrest in small pre-B cells (Bednarski et al., 2016). Thus, loss of BCLAF1 is expected to mitigate RAG DSB-induced inhibition of proliferation. Indeed, *Bclaf1*-deficient pre-B cells have increased cell cycle entry, and mice with B cell-specific deletion of BCLAF1 have increased numbers of proliferating, large pre-B cells, consistent with increased SYK activity. Loss of BCLAF1 does not result in a complete block in B cell development, which may reflect that additional mechanisms, such as p53, exist to regulate G1 arrest in small pre-B cells undergoing *Ig* gene rearrangement.

In summary, we find that SPIC/BCLAF1 functions to modulate PU.1 activity in pre-B cells. High activity of PU.1 promotes proliferation and expansion of large pre-B cells. As cells transition to small pre-B cell stage and initiate *Igl* gene assembly, RAG DSBs induce expression of SPIC, which partners with BCLAF1, to oppose PU.1 activity resulting in gene expression changes, including suppression of *Syk*, that promote transition from large to small pre-B cells. After rearrangement of *Igl* is completed and DSBs are repaired, termination of DDR signaling would result in cessation of SPIC/BCLAF1 activity and reestablishment of PU.1 transcriptional activation, which could support BCR signaling to drive transition to the immature B cell stage. We propose that RAG DSB-dependent activation of SPIC/BCLAF1 functions as rheostat to titer PU.1 activity during early B cell development.

STAR★METHODS

LEAD CONTACT AND MATERIALS AVAILABILITY

Further information and request for resources and reagents should be directed to the Lead Contact, Jeff Bednarski (bednarski_j@wustl.edu). All unique/stable reagents, including plasmids and mouse lines, are available from the Lead Contact with a completed Materials Transfer Agreement.

EXPERIMENTAL MODEL AND SUBJECT DETAILS

Mice: All mice were bred and maintained under specific pathogen-free conditions at the Washington University School of Medicine and were handled in accordance to the guidelines set forth by the Division of Comparative Medicine of Washington University. *Mb1-cre* (*cd79a*$^{tm1(cre)Reth}$) mice were purchased from The Jackson Laboratory. *Bclaf1*$^{f/f}$ mice were generated by the trans-NIH Knock-Out Mouse Project (KOMP) and obtained from the KOMP Repository (www.komp.org). *Rag1*$^{-/-}$*:μIgh:Bcl2* and *Art*$^{-/-}$*:μIgh:Bcl2* were generated as previously described (Bednarski et al., 2012, 2016). *Spic*$^{igfp/igfp}$ (*Spic*$^{tm2.1Kmm}$) were kindly provided by K. M. Murphy (Haldar et al., 2014). *Spic*$^{igfp/igfp}$, *Mb1-cre, Bclaf1*$^{f/f}$ and *Bclaf1*$^{f/f}$*:Mb1-cre* mice are on a B6 background. All other mice are on a mixed genetic background. Both sexes were used equivalently in all experiments. *In vivo* studies were conducted on 4–5 week old mice.

Cell Lines and Primary Cultures—*Rag1*$^{-/-}$*:Bcl2* and *Art*$^{-/-}$*:Bcl2* abl pre-B cells were a gift from Barry Sleckman. Cell lines were authenticated by genotyping. To induce cell cycle arrest and induction of RAG DSBs, cell lines were treated with 3 μM imatinib for indicated times (Bredemeyer et al., 2008). Primary pre-B cell cultures were generated by culturing bone marrow from 4–6 week old mice at 2×10^6 cells/mL in media containing 5 ng/mL of IL-7 (Miltenyi Biotec) for 7–10 days (Bednarski et al., 2012, 2016). Both sexes were used equivalently in all experiments. For IL-7 withdrawal experiments, cells were resuspended in media without IL-7 and maintained at 2×10^6 cells/mL for the indicated times. ATM inhibitor KU55933 (15 μM; Tocris) was added to cultures at time of addition of imatinib or IL-7 withdrawal.

METHOD DETAILS

cDNA Expression and shRNA-Mediated Knock-down—cDNAs for SPIC and PU.1 with 5′ FLAG-HA tag were individually cloned into the pFLRU-TRE-Ubc-rtTA-IRES-Thy1.2 lentiviral vector. shRNA targeting *Bclaf1* (sequence: 5′-CCTCATAGTCCTTCAC CTATT-3′) was cloned into the MSCV-hCD2-mir30 vector (Bednarski et al., 2012). Retrovirus was produced in platE cells by transfection of the retroviral plasmid with Lipofectamine 2000 (Life Technologies) according to the manufacturer's protocol. Lentivirus was produced in 293T cells by transfection of the lentiviral plasmid along with pCMV-VZV-G and pCMV-d8.2R plasmids with Lipofectamine 2000 (Stewart et al., 2003). Viral supernatant was collected and pooled from 24–72 hours after transfection. Viral supernatant was used immediately to transduce cells or was concentrated prior to transduction. To concentrate viral particles, PEG-8000 (Sigma; final concentration 8%) was added to viral supernatant followed by incubation at 4°C overnight and centrifugation at 2500 RPM for 20 minutes. Precipitated virus was resuspended at 300x concentration in sterile PBS. Pre-B cells were transduced with unconcentrated virus (10×10^6 cells in 1 mL viral supernatant) or with concentrated virus (40×10^6 in 1 mL with 10x viral particles) in media with polybrene (5 μg/ml; Sigma) by centrifugation for 90 min at 1300 RPM at room temperature. Four hours later fresh media was added and the cells were incubated overnight. Virus-containing media was removed and cells were cultured in fresh media (2×10^6/ml). Cells expressing the retrovirus construct were identified by flow cytometric assessment of hCD25 or hCD2 expression using a FACSCalibur (BD Biosciences). Transduced cells were sorted using biotin conjugated anti-hCD2 or anti-hCD25 (BD Biosciences) and anti-biotin magnetic beads (Miltenyi Biotec) on MS columns (Miltenyi Biotec) according to the manufacturer's protocol.

Flow Cytometric Analyses and Cell Sorting—Flow cytometric analyses were performed on a FACSCalibur or BD LSRFortessa (BD Biosciences). Sorting was conducted on a Sony Sy3200 through the Siteman Cancer Center Flow Cytometry Core Facility. Fluorescein isothiocyanate (FITC)-conjugated anti-CD45R/B220 (clone RA3–6B2), phycoerythrin (PE)-conjugated anti-CD43 (clone S7), FITC-conjugated anti-CD43 (clone S7), PE-Cy7-conjugated anti-CD45/B220 (clone RA3–6B2), allophycocyanin (APC)-conjugated anti-IgM (clone II/41), APC-conjugated anti-hCD2, and PE-conjugated anti-hCD2 were purchased from BD Biosciences. PE-conjugated anti-hCD25 (clone BC96) and APC-conjugated anti-hCD25 (clone BC96) were purchased from BioLegend.

Cell Cycle Analysis—To assess pre-BCR driven proliferation, pre-B cells were resuspended in media without IL-7 and maintained at 2×10^6 cells/mL. Twenty-four hours after removal from IL-7 cells were pulsed BrdU for two hours using the BrdU-FITC kit (BD Biosciences) per the manufacturer's instructions. DNA content was assessed by 7AAD (BD Biosciences).

Western Blot—Western blots were done on whole cell lysates (Bednarski et al., 2016). Anti-SYK (clone D1I5Q) and anti-GAPDH (clone D16H11) antibodies were from Cell Signaling Technology. Anti-BCLAF1 antibody (A300–608A) was from Bethyl Laboratories. Anti-PU.1 (PA5–17505) was from Thermo Fisher Scientific. Anti-FLAG (clone M2) was

from Sigma. Secondary reagents were horseradish peroxidase (HRP)-conjugated anti-mouse IgG (Cell Signaling; catalog # 7076) or anti-rabbit IgG (Cell Signaling; catalog # 7074). Westerns were developed with ECL (Pierce) and ECL Prime (GE Healthcare).

RT-PCR—For genomic DNA isolation, cells were lysed in lysis buffer (100 mM TRIS pH8.5, 5 mM EDTA, 200mM NaCl and 0.2% SDS) and DNA was precipitated by addition of isopropanol, washed with 70% ethanol and then resuspended in Tris-EDTA buffer (Bredemeyer et al., 2008). RNA was isolated using RNeasy (QIAGEN) and reversed transcribed using a polyT primer with SuperScriptII (Life Technologies) according to the manufacturers' protocol. RT-PCR was performed using Brilliant II SYBR Green (Agilent) and acquired on an Mx3000P (Stratagene). Each reaction was run in triplicate. Values were normalized to housekeeping genes as indicated, and fold change was determined by the ΔΔ cycle threshold method. Primer sequences are listed in Table S5.

Chromatin Immunoprecipitation (ChIP) and ChIP-Seq—ChIP was performed using anti-PU.1 (PA5-17505, Thermo Fisher Scientific), anti-FLAG (clone M2, Sigma), anti-HA (ab9110, Abcam), anti-BCLAF1 (A300-608A, Bethyl Laboratories), control rabbit IgG (Millipore) and control mouse IgG antibodies (clone P3.6.2.8.1, eBioscience) as previously described (Bednarski et al., 2016). Briefly, DNA was cross-linked with 2% formaldehyde for 10 min at room temp (1×10^6 cells/ml). Reaction was stopped with 125 μM Glycine. Cells were lysed with NP-40 and nuclei were frozen in liquid nitrogen then lysed with SDS. DNA was fragmented by sonicating with 30 s pulses for 60 cycles using a Bioruptor (Diagenode). DNA fragmentation was in the range of 200–500 bp and was monitored by agarose gel electrophoresis. Immunoprecipitation was performed with anti-PU.1 (1:100), anti-HA (1 μg), anti-BCLAF1 (2 μg), or control rabbit IgG and Protein A Dynabeads (Life Technologies). DNA was eluted, reverse cross-linked and then purified with QIAquick PCR purification kit (QIAGEN). For ChIP-PCR analysis, PCR was performed using Brilliant II SYBR Green (Agilent) and acquired on an Mx3000P (Stratagene). Primers are listed in Table S5. For ChIP-seq analysis, fragmented DNA was quantified using 2100 Bioanalyzer (Agilent Technologies) and DNA libraries were prepared using Illumina TruSeq. Sequencing was performed using an Illumina HiSeq 3000 by the Washington University Genome Technology Access Center. Input controls were used for all samples. FASTQ files were aligned to mm9 using Map with Bowtie for Illumina v. 1.1.2 to the reference genome (NCBI37/mm9) (Langmead and Salzberg, 2012). MACS version 2 was used to call peaks with a tag size set to 45, band width of 300 and a p value of 1×10^{-5} (Zhang et al., 2008). Input. bed files of total reads for MM-ChIP were generated using Convert from BAM to BED tool v0.1.0 in Galaxy V18.09 (Afgan et al., 2016). Promoter regions were defined as regions extending 12 kb upstream of transcription start site. R package (GenomicRanges) and Bedtools V2.25.0 were used to determine overlapping ChIP peaks (Lawrence et al., 2013; Quinlan and Hall, 2010). MAnorm using parameters -w 300-s1 50-s2 50 was used to calculate normalized fold changes for each ChIP-seq comparison (Shao et al., 2012). A 1.5 fold change magnitude was used to separate enriched and unbiased peaks for each comparison. EaSeq v1.111 was used to generate ratiometric heatmaps from RPM-normalized ChIP-seq signal (Lerdrup et al., 2016). Data will be deposited in NCBI's Gene Expression Omnibus.

Ultra-Low-Input Native ChIP—EGFP-negative (−) and EGFP-expressing (+) small pre-B cells were sorted from *SPIC*$^{igfp/igfp}$ mice. ULI-NChIP was performed as previously described (Brind'Amour et al., 2015). Briefly, chromatin was fragmented using micrococcal nuclease (New England Biolabs) at 37°C for 5 mins and diluted in complete immunoprecipitation buffer (20mM Tris-HCl pH 8.0, 2mM EDTA, 15mM NaCl, 0.1% Triton X-100, protease and phosphatase inhibitors). Fragmented chromatin was precleared with Protein A Dynabeads (Life Technologies). Immunoprecipitation was performed with anti-PU.1 (1:100), anti-BCLAF1 (10 μg), or control rabbit IgG and Protein A Dynabeads (Life Technologies). The antibody-beads complex was washed with low salt (20mM Tris-HCl, pH 8.0, 0.1%SDS, 1% Triton X-100, 0.1% deoxycholate, 2mM EDTA and 150mM NaCl) and high salt (20mM Tris-HCl, pH 8.0, 0.1%SDS, 1% Triton X-100, 0.1% deoxycholate, 2mM EDTA and 300mM NaCl) buffer. DNA was eluted in high salt buffer. DNA was purified and ChIP-PCR was performed as above.

RNA-Seq Analysis—RNA was extracted using RNeasy Kit (QIAGEN). Libraries were prepared using Illumina TrueSeq Adpaters and paired-end sequencing was performed using an Illumina HiSeq 3000 by the Washington University Genome Technology Access Center according to the manufacturer's protocols. Sequencing data were analyzed as previously described (Andley et al., 2018). Briefly, RNA-seq reads were aligned to mm9 assembly with STAR version 2.0.4b1. Gene counts were derived from uniquely aligned unambiguous reads by Subread-featureCount version 1.4.5. Gene-level counts were imported into the R/Bioconductor package EdgeR and TMM normalization size factors were calculated to adjust for differences in library size (Robinson et al., 2010). Differential expression analysis was then performed to analyze for differences between conditions using the R/Bioconductor package limma-voom (Law et al., 2014). Results were filtered for only those genes with Benjamini-Hochberg false-discovery rate adjusted p values less than or equal to 0.05. DAVID (Database for Annotation, Visualization and Integrated Discovery, v6.8) was used to test if differentially expressed genes resulted in perturbations in known Gene Ontology (GO) terms and KEGG pathways (Huang et al., 2009). Volcano plots were generated using R (ggplot2). Java TreeView Version 1.1.6r4 and R/Bioconductor package heatmap3 were used to display heat-maps (Saldanha, 2004; Zhao et al., 2014). DAVID was used to display annotated KEGG graphs across groups of samples for each GO term or KEGG pathway with a Benjamini-Hochberg false-discovery rate adjusted p value ≤ 0.05.

Tandem Affinity Purification and MS Analysis—FLAG-HA-tagged SPIC and PU.1 were immunoprecipitated using anti-FLAG antibody as previously described with the following modifications (Mosammaparast et al., 2013; Nakatani and Ogryzko, 2003). Cells were lysed lysis of cells (1×10^9 cells/1.5 ml) in TAP buffer (50 mM Tris, pH 7.9,150 mM NaCI, 1% NP-40, and protease and phosphatase inhibitor cocktails (Sigma). The lysate was cleared by centrifugation and incubated with anti-FLAG beads (40 μl/10^9 cells; clone M2; Sigma-Aldrich) for 4 hours. After extensive washing in the same buffer, bound material was eluted with FLAG peptide (Sigma-Aldrich) and analyzed by western blotting. Coomassie-stained bands were cut from SDS-PAGE and sent to Taplin Biological Mass Spectrometry Facility at Harvard Medical School (taplin.med.harvard.edu). In-gel trypsin digestion was performed and the detection of complexed proteins was done using Orbitrap ion-trap mass

spectrometers (ThermoFisher Scientific). Interacting proteins were identified by matching protein database with acquired fragmentation pattern by using Sequest (ThermoFisher Scientific) (Eng et al., 1994).

QUANTIFICATION AND STATISTICAL ANALYSIS

RNA-seq and ChIP-seq were analyzed for statistical significance using the software packages described above. For all other analyses, statistics and figures were generated using Prism 8 (v8.0.2). P values were generated via Student's t test (unpaired, two-tailed). Error bars are SE. *p value ≤ 0.05, **p value ≤ 0.01, ***p value ≤ 0.001, ****p value ≤ 0.0001.

DATA AND CODE AVAILABILITY

The ChIP-seq and RNA-seq data generated during this study are available at NCBI Gene Expression Omnibus under accession number GEO: GSE129130.

Supplementary Material

Refer to Web version on PubMed Central for supplementary material.

ACKNOWLEDGMENTS

This work was supported by NIH grants K08 AI102946 (J.J.B.), R01 CA193318 (N.M.), R01 CA227001 (N.M.), and R01 CA188286 (J.E.P.). J.J.B. is supported by the Alex's Lemonade Stand Foundation, the Foundation for Barnes-Jewish Hospital Cancer Frontier Fund, the Barnard Trust, and an American Society of Hematology Scholar Award. N.M. is an American Cancer Society Research Scholar and is supported by the Alvin J. Siteman Cancer Research Fund. We thank the Genome Technology Access Center (P30 CA91842 and UL1 TR000448) at Washington University School of Medicine for assistance with experiments. NIH grants to Regeneron (U01HG004085) and the CSD Consortium (U01HG004080) funded the KOMP Program.

REFERENCES

Afgan E, Baker D, van den Beek M, Blankenberg D, Bouvier D, Čech M, Chilton J, Clements D, Coraor N, Eberhard C, et al. (2016). The Galaxy platform for accessible, reproducible and collaborative biomedical analyses: 2016 update. Nucleic Acids Res. 44 (W1), W3–W10. [PubMed: 27137889]

Anderson MK, Weiss AH, Hernandez-Hoyos G, Dionne CJ, and Rothenberg EV (2002). Constitutive expression of PU.1 in fetal hematopoietic progenitors blocks T cell development at the pro-T cell stage. Immunity 16, 285–296. [PubMed: 11869688]

Andley UP, Tycksen E, McGlasson-Naumann BN, and Hamilton PD (2018). Probing the changes in gene expression due to α-crystallin mutations in mouse models of hereditary human cataract. PLoS ONE 13, e0190817. [PubMed: 29338044]

Back J, Allman D, Chan S, and Kastner P (2005). Visualizing PU.1 activity during hematopoiesis. Exp. Hematol 33, 395–402. [PubMed: 15781329]

Batista CR, Li SK, Xu LS, Solomon LA, and DeKoter RP (2017). PU.1 regulates Ig light chain transcription and rearrangement in pre-B cells during B cell development. J. Immunol 198, 1565–1574. [PubMed: 28062693]

Bednarski JJ, Nickless A, Bhattacharya D, Amin RH, Schlissel MS, and Sleckman BP (2012). RAG-induced DNA double-strand breaks signal through Pim2 to promote pre-B cell survival and limit proliferation. J. Exp. Med 209, 11–17. [PubMed: 22201128]

Bednarski JJ, Pandey R, Schulte E, White LS, Chen BR, Sandoval GJ, Kohyama M, Haldar M, Nickless A, Trott A, et al. (2016). RAG-mediated DNA double-strand breaks activate a cell type-specific checkpoint to inhibit pre-B cell receptor signals. J. Exp. Med 213, 209–223. [PubMed: 26834154]

Bemark M, Mårtensson A, Liberg D, and Leanderson T (1999). Spi-C, a novel Ets protein that is temporally regulated during B lymphocyte development. J. Biol. Chem 274, 10259–10267. [PubMed: 10187812]

Brass AL, Kehrli E, Eisenbeis CF, Storb U, and Singh H (1996). Pip, a lymphoid-restricted IRF, contains a regulatory domain that is important for autoinhibition and ternary complex formation with the Ets factor PU.1. Genes Dev. 10, 2335–2347. [PubMed: 8824592]

Bredemeyer AL, Helmink BA, Innes CL, Calderon B, McGinnis LM, Mahowald GK, Gapud EJ, Walker LM, Collins JB, Weaver BK, et al. (2008). DNA double-strand breaks activate a multi-functional genetic program in developing lymphocytes. Nature 456, 819–823. [PubMed: 18849970]

Brind'Amour J, Liu S, Hudson M, Chen C, Karimi MM, and Lorincz MC (2015). An ultra-low-input native ChIP-seq protocol for genome-wide profiling of rare cell populations. Nat. Commun 6, 6033. [PubMed: 25607992]

Carlsson R, Persson C, and Leanderson T (2003). SPI-C, a PU-box binding ETS protein expressed temporarily during B-cell development and in macrophages, contains an acidic transactivation domain located to the N-terminus. Mol. Immunol 39, 1035–1043. [PubMed: 12749910]

Clark MR, Mandal M, Ochiai K, and Singh H (2014). Orchestrating B cell lymphopoiesis through interplay of IL-7 receptor and pre-B cell receptor signalling. Nat. Rev. Immunol 14, 69–80. [PubMed: 24378843]

Dakic A, Wu L, and Nutt SL (2007). Is PU.1 a dosage-sensitive regulator of haemopoietic lineage commitment and leukaemogenesis? Trends Immunol. 28, 108–114. [PubMed: 17267285]

DeKoter RP, Lee HJ, and Singh H (2002). PU.1 regulates expression of the interleukin-7 receptor in lymphoid progenitors. Immunity 16, 297–309. [PubMed: 11869689]

DeMicco A, Reich T, Arya R, Rivera-Reyes A, Fisher MR, and Bassing CH (2016). Lymphocyte lineage-specific and developmental stage specific mechanisms suppress cyclin D3 expression in response to DNA double strand breaks. Cell Cycle 15, 2882–2894. [PubMed: 27327568]

Desiderio S, Lin WC, and Li Z (1996). The cell cycle and V(D)J recombination. Curr. Top. Microbiol. Immunol 217, 45–59. [PubMed: 8787617]

Eng JK, McCormack AL, and Yates JR (1994). An approach to correlate tandem mass spectral data of peptides with amino acid sequences in a protein database. J. Am. Soc. Mass Spectrom 5, 976–989. [PubMed: 24226387]

Fugmann SD, Lee AI, Shockett PE, Villey IJ, and Schatz DG (2000). The RAG proteins and V(D)J recombination: complexes, ends, and transposition. Annu. Rev. Immunol 18, 495–527. [PubMed: 10837067]

Haldar M, Kohyama M, So AY-L, Wumesh KC, Wu X, Briseno CG, Satpathy AT, Kretzer NM, Rajasekaran NS, Wang L, et al. (2014). Heme-mediated BACH1 degradation induces SPI-C to promote monocyte differentiation into iron-recycling macrophages. Cell 156, 1223–1234. [PubMed: 24630724]

Hashimoto S, Nishizumi H, Hayashi R, Tsuboi A, Nagawa F, Takemori T, and Sakano H (1999). Prf, a novel Ets family protein that binds to the PU.1 binding motif, is specifically expressed in restricted stages of B cell development. Int. Immunol 11, 1423–1429. [PubMed: 10464163]

Heinz S, Benner C, Spann N, Bertolino E, Lin YC, Laslo P, Cheng JX, Murre C, Singh H, and Glass CK (2010). Simple combinations of lineage-determining transcription factors prime cis-regulatory elements required for macrophage and B cell identities. Mol. Cell 38, 576–589. [PubMed: 20513432]

Helmink BA, and Sleckman BP (2012). The response to and repair of RAG-mediated DNA double-strand breaks. Annu. Rev. Immunol 30, 175–202. [PubMed: 22224778]

Herzog S, Reth M, and Jumaa H (2009). Regulation of B-cell proliferation and differentiation by pre-B-cell receptor signalling. Nat. Rev. Immunol 9, 195–205. [PubMed: 19240758]

Hobeika E, Thiemann S, Storch B, Jumaa H, Nielsen PJ, Pelanda R, and Reth M (2006). Testing gene function early in the B cell lineage in mb1-cre mice. Proc. Natl. Acad. Sci. U S A 103, 13789–13794. [PubMed: 16940357]

Huang D, Sherman BT, Zheng X, Yang J, Imamichi T, Stephens R, and Lempicki RA (2009). Extracting biological meaning from large gene lists with DAVID. Curr. Protoc. Bioinformatics Chapter 13, Unit 13.11.

Johnson K, Hashimshony T, Sawai CM, Pongubala JM, Skok JA, Aifantis I, and Singh H (2008). Regulation of immunoglobulin light-chain recombination by the transcription factor IRF-4 and the attenuation of interleukin-7 signaling. Immunity 28, 335–345. [PubMed: 18280186]

Kasof GM, Goyal L, and White E (1999). Btf, a novel death-promoting transcriptional repressor that interacts with Bcl-2-related proteins. Mol. Cell. Biol 19, 4390–4404. [PubMed: 10330179]

Langmead B, and Salzberg SL (2012). Fast gapped-read alignment with Bowtie 2. Nat. Methods 9, 357–359. [PubMed: 22388286]

Law CW, Chen Y, Shi W, and Smyth GK (2014). voom: Precision weights unlock linear model analysis tools for RNA-seq read counts. Genome Biol. 15, R29. [PubMed: 24485249]

Lawrence M, Huber W, Pagès H, Aboyoun P, Carlson M, Gentleman R, Morgan MT, and Carey VJ (2013). Software for computing and annotating genomic ranges. PLoS Comput. Biol 9, e1003118. [PubMed: 23950696]

Lerdrup M, Johansen JV, Agrawal-Singh S, and Hansen K (2016). An interactive environment for agile analysis and visualization of ChIP-sequencing data. Nat. Struct. Mol. Biol 23, 349–357. [PubMed: 26926434]

Li SK, Solomon LA, Fulkerson PC, and DeKoter RP (2015). Identification of a negative regulatory role for Spi-C in the murine B cell lineage. J. Immunol 194, 3798–3807. [PubMed: 25769919]

Liu H, Lu ZG, Miki Y, and Yoshida K (2007). Protein kinase C delta induces transcription of the TP53 tumor suppressor gene by controlling death-promoting factor Btf in the apoptotic response to DNA damage. Mol. Cell. Biol 27, 8480–8491. [PubMed: 17938203]

Lu R, Medina KL, Lancki DW, and Singh H (2003). IRF-4,8 orchestrate the pre-B-to-B transition in lymphocyte development. Genes Dev. 17, 1703–1708. [PubMed: 12832394]

Ma S, Turetsky A, Trinh L, and Lu R (2006). IFN regulatory factor 4 and 8 promote Ig light chain kappa locus activation in pre-B cell development. J. Immunol 177, 7898–7904. [PubMed: 17114461]

Maitra S, and Atchison M (2000). BSAP can repress enhancer activity by targeting PU.1 function. Mol. Cell. Biol 20, 1911–1922. [PubMed: 10688639]

McPherson JP, Sarras H, Lemmers B, Tamblyn L, Migon E, Matysiak-Zablocki E, Hakem A, Azami SA, Cardoso R, Fish J, et al. (2009). Essential role for Bclaf1 in lung development and immune system function. Cell Death Differ. 16, 331–339. [PubMed: 19008920]

Mosammaparast N, Kim H, Laurent B, Zhao Y, Lim HJ, Majid MC, Dango S, Luo Y, Hempel K, Sowa ME, et al. (2013). The histone demethylase LSD1/KDM1A promotes the DNA damage response. J. Cell Biol 203, 457–470. [PubMed: 24217620]

Nakatani Y, and Ogryzko V (2003). Immunoaffinity purification of mammalian protein complexes. Methods Enzymol. 370, 430–444. [PubMed: 14712665]

Nerlov C, Querfurth E, Kulessa H, and Graf T (2000). GATA-1 interacts with the myeloid PU.1 transcription factor and represses PU.1-dependent transcription. Blood 95, 2543–2551. [PubMed: 10753833]

Nutt SL, Metcalf D, D'Amico A, Polli M, and Wu L (2005). Dynamic regulation of PU.1 expression in multipotent hematopoietic progenitors. J. Exp. Med 201, 221–231. [PubMed: 15657291]

Ochiai K, Maienschein-Cline M, Mandal M, Triggs JR, Bertolino E, Sciammas R, Dinner AR, Clark MR, and Singh H (2012). A self-reinforcing regulatory network triggered by limiting IL-7 activates pre-BCR signaling and differentiation. Nat. Immunol 13, 300–307. [PubMed: 22267219]

Pang SH, Carotta S, and Nutt SL (2014). Transcriptional control of pre-B cell development and leukemia prevention. Curr. Top. Microbiol. Immunol 381, 189–213. [PubMed: 24831348]

Pang SH, Minnich M, Gangatirkar P, Zheng Z, Ebert A, Song G, Dickins RA, Corcoran LM, Mullighan CG, Busslinger M, et al. (2016). PU.1 cooperates with IRF4 and IRF8 to suppress pre-B-cell leukemia. Leukemia 30, 1375–1387. [PubMed: 26932576]

Pang SHM, de Graaf CA, Hilton DJ, Huntington ND, Carotta S, Wu L, and Nutt SL (2018). PU.1 is required for the developmental progression of multipotent progenitors to common lymphoid progenitors. Front. Immunol 9, 1264. [PubMed: 29942304]

Polli M, Dakic A, Light A, Wu L, Tarlinton DM, and Nutt SL (2005). The development of functional B lymphocytes in conditional PU.1 knock-out mice. Blood 106, 2083–2090. [PubMed: 15933053]

Pongubala JM, Nagulapalli S, Klemsz MJ, McKercher SR, Maki RA, and Atchison ML (1992). PU.1 recruits a second nuclear factor to a site important for immunoglobulin kappa 3′ enhancer activity. Mol. Cell. Biol 12, 368–378. [PubMed: 1729611]

Qin C, Zhang R, Lang Y, Shao A, Xu A, Feng W, Han J, Wang M, He W, Yu C, and Tang J (2019). Bclaf1 critically regulates the type I interferon response and is degraded by alphaherpesvirus US3. PLoS Pathog. 15, e1007559. [PubMed: 30682178]

Quinlan AR, and Hall IM (2010). BEDTools: a flexible suite of utilities for comparing genomic features. Bioinformatics 26, 841–842. [PubMed: 20110278]

Rajewsky K (1996). Clonal selection and learning in the antibody system. Nature 381, 751–758. [PubMed: 8657279]

Robinson MD, McCarthy DJ, and Smyth GK (2010). edgeR: a Bioconductor package for differential expression analysis of digital gene expression data. Bioinformatics 26, 139–140. [PubMed: 19910308]

Rogers JH, Owens KS, Kurkewich J, Klopfenstein N, Iyer SR, Simon MC, and Dahl R (2016). E2A antagonizes PU.1 activity through inhibition of DNA binding. BioMed Res. Int 2016, 3983686. [PubMed: 26942192]

Rolink A, Kudo A, Karasuyama H, Kikuchi Y, and Melchers F (1991). Long-term proliferating early pre B cell lines and clones with the potential to develop to surface Ig-positive, mitogen reactive B cells in vitro and in vivo. EMBO J. 10, 327–336. [PubMed: 1991449]

Rolink AG, Winkler T, Melchers F, and Andersson J (2000). Precursor B cell receptor-dependent B cell proliferation and differentiation does not require the bone marrow or fetal liver environment. J. Exp. Med 191, 23–32. [PubMed: 10620602]

Rosenbauer F, Wagner K, Kutok JL, Iwasaki H, Le Beau MM, Okuno Y, Akashi K, Fiering S, and Tenen DG (2004). Acute myeloid leukemia induced by graded reduction of a lineage-specific transcription factor, PU.1. Nat. Genet 36, 624–630. [PubMed: 15146183]

Rosenbauer F, Owens BM, Yu L, Tumang JR, Steidl U, Kutok JL, Clayton LK, Wagner K, Scheller M, Iwasaki H, et al. (2006). Lymphoid cell growth and transformation are suppressed by a key regulatory element of the gene encoding PU.1. Nat. Genet 38, 27–37. [PubMed: 16311598]

Saldanha AJ (2004). Java Treeview—extensible visualization of microarray data. Bioinformatics 20, 3246–3248. [PubMed: 15180930]

Savage KI, Gorski JJ, Barros EM, Irwin GW, Manti L, Powell AJ, Pellagatti A, Lukashchuk N, McCance DJ, McCluggage WG, et al. (2014). Identification of a BRCA1-mRNA splicing complex required for efficient DNA repair and maintenance of genomic stability. Mol. Cell 54, 445–459. [PubMed: 24746700]

Schwarzenbach H, Newell JW, and Matthias P (1995). Involvement of the Ets family factor PU.1 in the activation of immunoglobulin promoters. J. Biol. Chem 270, 898–907. [PubMed: 7822329]

Schweitzer BL, and DeKoter RP (2004). Analysis of gene expression and Ig transcription in PU.1/Spi-B-deficient progenitor B cell lines. J. Immunol 172, 144–154. [PubMed: 14688320]

Scott EW, Simon MC, Anastasi J, and Singh H (1994). Requirement of transcription factor PU.1 in the development of multiple hematopoietic lineages. Science 265, 1573–1577. [PubMed: 8079170]

Scott EW, Fisher RC, Olson MC, Kehrli EW, Simon MC, and Singh H (1997). PU.1 functions in a cell-autonomous manner to control the differentiation of multipotential lymphoid-myeloid progenitors. Immunity 6, 437–447. [PubMed: 9133423]

Shao Z, Zhang Y, Yuan GC, Orkin SH, and Waxman DJ (2012). MAnorm: a robust model for quantitative comparison of ChIP-Seq data sets. Genome Biol. 13, R16. [PubMed: 22424423]

Shao AW, Sun H, Geng Y, Peng Q, Wang P, Chen J, Xiong T, Cao R, and Tang J (2016). Bclaf1 is an important NF-κB signaling transducer and C/EBPβ regulator in DNA damage-induced senescence. Cell Death Differ. 23, 865–875. [PubMed: 26794446]

Sokalski KM, Li SK, Welch I, Cadieux-Pitre HA, Gruca MR, and DeKoter RP (2011). Deletion of genes encoding PU.1 and Spi-B in B cells impairs differentiation and induces pre-B cell acute lymphoblastic leukemia. Blood 118, 2801–2808. [PubMed: 21768304]

Solomon LA, Li SK, Piskorz J, Xu LS, and DeKoter RP (2015). Genome-wide comparison of PU.1 and Spi-B binding sites in a mouse B lymphoma cell line. BMC Genomics 16, 76. [PubMed: 25765478]

Steinel NC, Lee BS, Tubbs AT, Bednarski JJ, Schulte E, Yang-Iott KS, Schatz DG, Sleckman BP, and Bassing CH (2013). The ataxia telangiectasia mutated kinase controls Igκ allelic exclusion by inhibiting secondary Vκ-to-Jκ rearrangements. J. Exp. Med 210, 233–239. [PubMed: 23382544]

Stewart SA, Dykxhoorn DM, Palliser D, Mizuno H, Yu EY, An DS, Sabatini DM, Chen IS, Hahn WC, Sharp PA, et al. (2003). Lentivirus-delivered stable gene silencing by RNAi in primary cells. RNA 9, 493–501. [PubMed: 12649500]

Su GH, Chen HM, Muthusamy N, Garrett-Sinha LA, Baunoch D, Tenen DG, and Simon MC (1997). Defective B cell receptor-mediated responses in mice lacking the Ets protein, Spi-B. EMBO J. 16, 7118–7129. [PubMed: 9384589]

Vohhodina J, Barros EM, Savage AL, Liberante FG, Manti L, Bankhead P, Cosgrove N, Madden AF, Harkin DP, and Savage KI (2017). The RNA processing factors THRAP3 and BCLAF1 promote the DNA damage response through selective mRNA splicing and nuclear export. Nucleic Acids Res. 45, 12816–12833. [PubMed: 29112714]

Wossning T, Herzog S, Köhler F, Meixlsperger S, Kulathu Y, Mittler G, Abe A, Fuchs U, Borkhardt A, and Jumaa H (2006). Deregulated Syk inhibits differentiation and induces growth factor-independent proliferation of pre-B cells. J. Exp. Med 208, 2829–2840.

Ye M, Ermakova O, and Graf T (2005). PU.1 is not strictly required for B cell development and its absence induces a B-2 to B-1 cell switch. J. Exp. Med 202, 1411–1422. [PubMed: 16301746]

Zhang Y, Liu T, Meyer CA, Eeckhoute J, Johnson DS, Bernstein BE, Nusbaum C, Myers RM, Brown M, Li W, and Liu XS (2008). Model-based analysis of ChIP-seq (MACS). Genome Biol. 9, R137. [PubMed: 18798982]

Zhao S, Guo Y, Sheng Q, and Shyr Y (2014). Advanced heat map and clustering analysis using heatmap3. BioMed Res. Int 2014, 986048. [PubMed: 25143956]

Zhu X, Schweitzer BL, Romer EJ, Sulentic CE, and DeKoter RP (2008). Transgenic expression of Spi-C impairs B-cell development and function by affecting genes associated with BCR signaling. Eur. J. Immunol 38, 2587–2599. [PubMed: 18792411]

Highlights

- RAG DNA breaks upregulate SPIC, which induces genome-wide changes in PU.1 activity
- SPIC binds to gene-regulatory elements, resulting in loss of PU.1 at these regions
- SPIC complexes with BCLAF1 to suppress transcription in response to RAG DNA breaks
- SPIC/BCLAF1 inhibits SYK and promotes transition from large to small pre-B cells

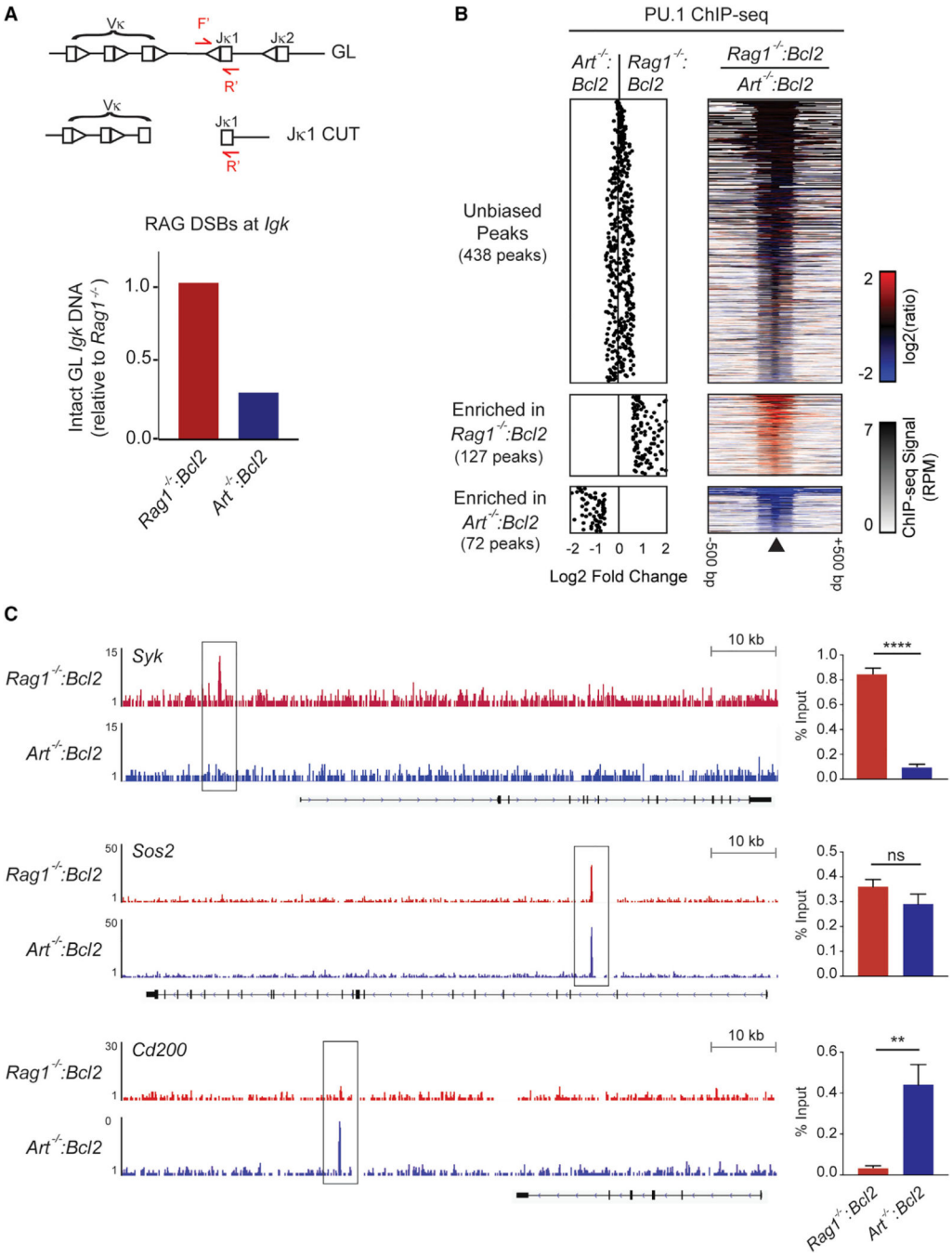

Figure 1. RAG DSB Signals Induce Genome-wide Changes in PU.1 Binding

(A) qPCR analysis of *Igk* genomic DNA from *Rag1*$^{-/-}$*:Bcl2* (red) and *Art*$^{-/-}$*:Bcl2* (blue) abl pre-B cells treated with imatinib for 48 h. Schematic shows germline (GL) *Igk* locus and unrepaired Jκ1 coding end with location of PCR primers. PCR is normalized to *Rag1*$^{-/-}$*:Bcl2* abl pre-B cells, which do not generate RAG DSBs and have only intact germline *Igk* DNA. Data are representative of three independent experiments.

(B) Dot plot and heatmap of fold changes and signal Intensity for PU.1 peaks Identified by ChIP-seq In *Rag1*$^{-/-}$*:Bcl2* and *Art*$^{-/-}$*:Bcl2* abl pre-B cells treated with Imatinib for 48 h. Data are from common peaks identified in two replicates for each cell.

(C) Representative tracks at indicated regions for PU.1 ChIP-seq from (B). ChIP-qPCR validation for PU.1 binding at each locus is also shown. Data are mean and SE for three independent experiments. **$p \leq 0.01$ and ****$p \leq 0.0001$; ns, not significant.

See also Figure S1.

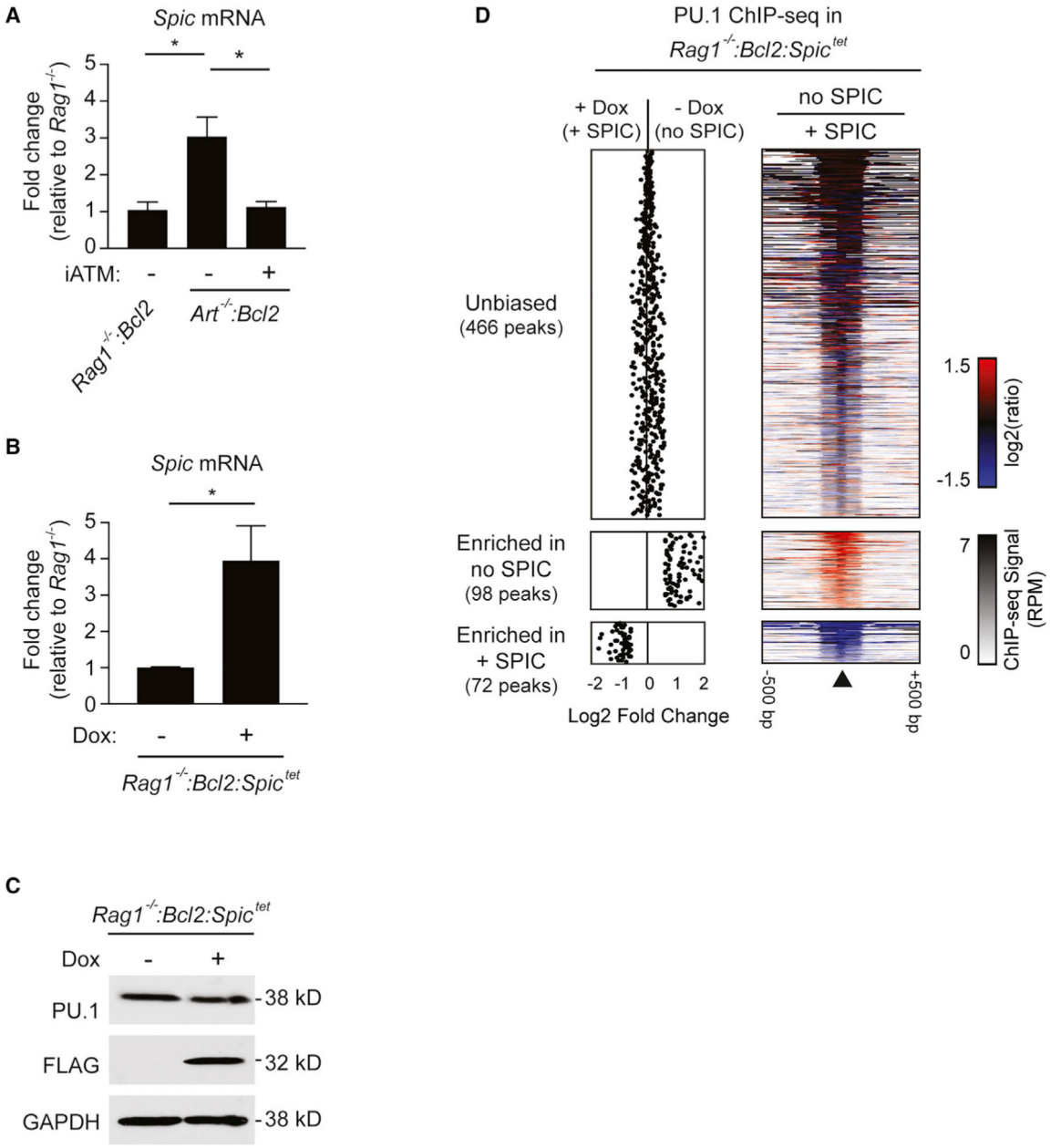

Figure 2. Expression of SPIC Alters PU.1 Binding

(A) *Spic* mRNA expression in *Rag1*$^{-/-}$*:Bcl2* and *Art*$^{-/-}$*:Bcl2* ablpre-B cells treated with imatinib for 48 h. *Art*$^{-/-}$*:Bcl2* ablpre-B cells were also treated with vehicle (−) or 15 μM ATM inhibitor KU55933 (+ iATM). Data are relative to *Rag1*$^{-/-}$*:Bcl2* and are mean and SE for three independent experiments.

(B) *Spic* mRNA expression in *Rag1*$^{-/-}$*:Bcl2:Spic*^{tet} abl pre-B cells treated with imatinib alone (−) or with imatinib and 2 μM doxycycline (Dox; +) for 48 h. Data are relative to *Rag1*$^{-/-}$*:Bcl2:Spic*^{tet} without doxycycline and are mean and SE for three independent experiments.

(C) Western blot shows PU.1 and SPIC (determined by anti-FLAG antibody) in *Rag1*$^{-/-}$*:Bcl2:Spic*^{tet} abl pre-B cells treated as in (B). Data are representative of three independent experiments.

(D) Dot plot and heatmap of fold changes and signal intensity for PU.1 peaks identified by ChIP-seq in *Rag1* $^{-/-}$*:Bcl2:Spic*^{tet} abl pre-B cells treated with imatinib alone (− Dox, no SPIC) or with imatinib and 2 μM doxycycline (+ Dox, + SPIC) for 48 h as in (B). Data are from common peaks identified in two replicates for each cell line.

*$p \leq 0.05$.

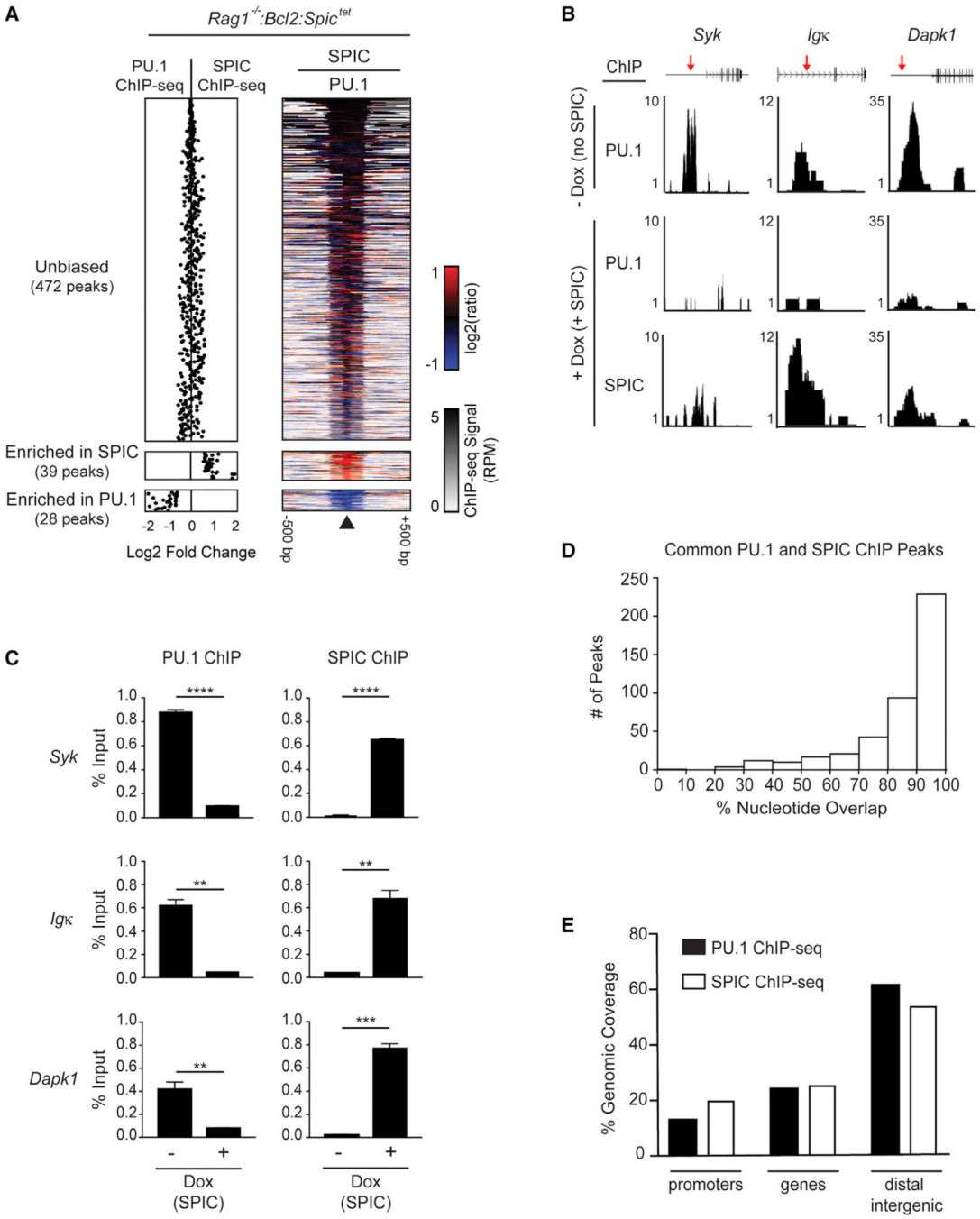

Figure 3. SPIC and PU.1 Bind to Identical Genomic Regions

(A) Dot plot and heatmap of fold changes and signal intensity for PU.1 and SPIC (by anti-HA ChIP) peaks identified by ChIP-seq in *Rag1*$^{-/-}$*:Bcl2:Spic*^{tet} abl pre-B cells treated with imatinib for 48 h in the absence (for PU.1 ChIP) or presence (for SPIC ChIP) of 2 μM doxycycline (Dox). Data are from common peaks identified in two replicates of each cell line.

(B) Representative ChIP-seq binding of PU.1 and SPIC at indicated regions. PU.1 ChIP-seq was performed in *Rag1*$^{-/-}$*:Bcl2:Spic*^{tet} abl pre-B cells treated with imatinib alone (− Dox, no

SPIC) or with imatinib and doxycycline to induce expression of SPIC(+ Dox, + SPIC) for 48 h. ChIP-seq for SPIC was performed as in A in *Rag1*$^{-/-}$*:Bd2:Spic*^{tet} abl pre-B cells treated with imatinib and doxycycline for 48 h.

(C) ChIP-qPCR validation for PU.1 and SPIC binding at each locus shown in (B). Data are mean and SE for three independent experiments. **p ≤ 0.01, ***p ≤ 0.001, and ****p ≤ 0.0001.

(D) Nucleotide overlap between PU.1 and SPIC peaks identified in (A). Peaks were grouped in bins on the basis of percentage of overlap as shown.

(E) Enrichment of PU.1 and SPIC binding across genomic regions on the basis of ChIP-seq data in (A).

See also Figure S2.

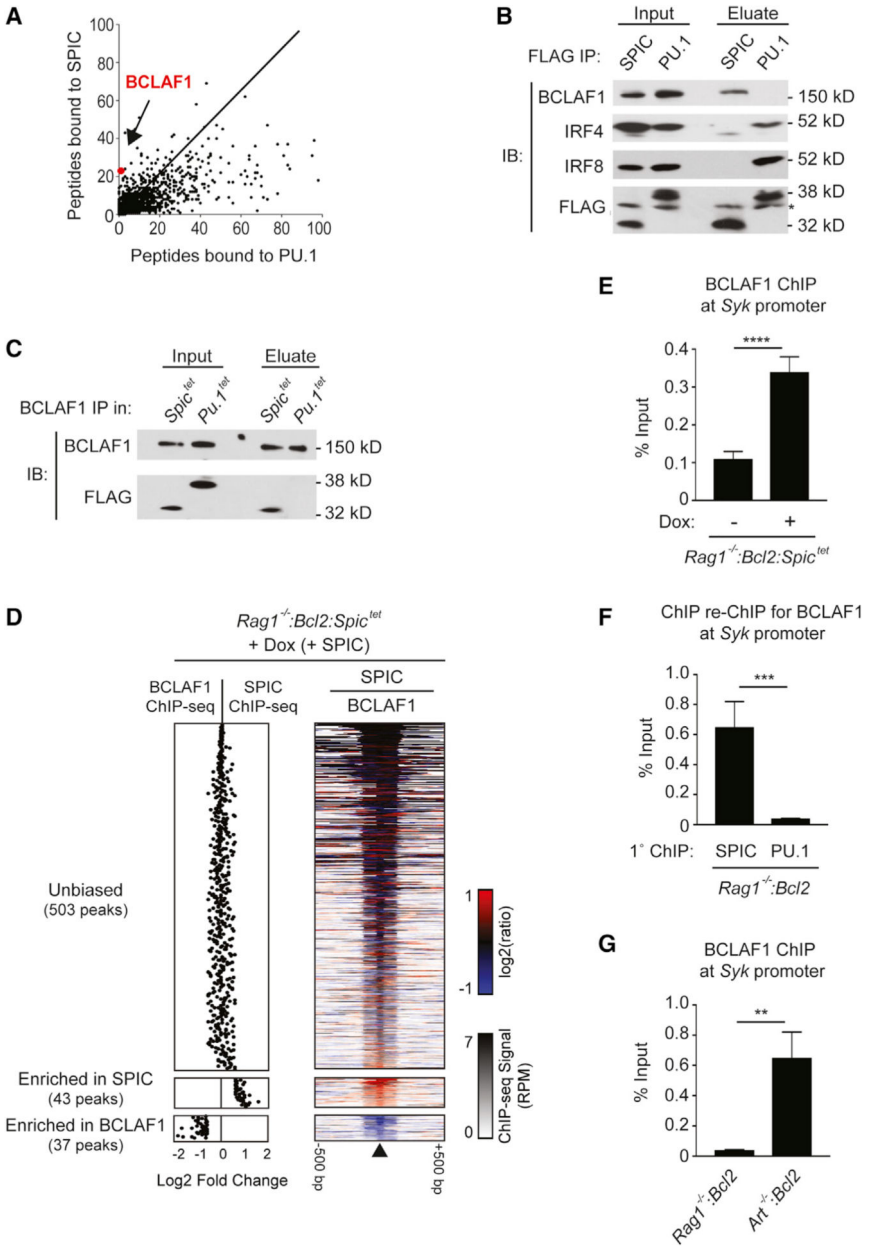

Figure 4. SPIC Recruits BCLAF1 to Chromatin

(A) FLAG-HA-SPIC and FLAG-HA-PU.1 were immunoprecipitated from *Art*$^{-/-}$*:Bcl2:Spic*^{tet} and *Art*$^{-/-}$*:Bcl2:Pu.1*^{tet}, respectively, after treatment with imatinib and 2 μM doxycycline for 48 h. Scatterplot shows number of total peptides per protein identified by mass spectrometry analysis of co-immunoprecipitation of SPIC (y axis) versus PU.1 (x axis).

(B) FLAG-HA-tagged SPIC and FLAG-HA-tagged PU.1 were immunoprecipitated from *Art*$^{-/-}$*:Bcl2: Spic*^{tet} and *Art*$^{-/-}$*:Bcl2:Pu.1*^{tet} abl pre-B cells, respectively, treated as in (A). IP samples were immunoblotted (IB) for BCLAF1, IRF4, IRF8, and FLAG. Asterisk indicates non-specific band.

(C) BCLAF1 was immunoprecipitated from *Art*$^{-/-}$*:Bcl2:Spic*^{tet} (*Spic*^{tet}) and *Art*$^{-/-}$*:Bcl2:Pu.1*^{tet} (*Pu.1*^{tet}) abl pre-B cells treated as in (A). IP samples were immunoblotted for BCLAF1 and FLAG.

(D) Dot plot and heatmap of fold changes and signal intensity for BCLAF1 and SPIC peaks (by anti-HA ChIP as in Figure 3A) identified by ChIP-seq in *Rag1*$^{-/-}$*:Bcl2:Spic*^{tet} abl pre-B cells treated with imatinib and 2 μM doxycycline for 48 h. Data are from common peaks identified in two replicates of each cell line.

(E) ChIP-qPCR of BCLAF1 binding at the *Syk* promoter in *Rag1*$^{-/-}$*:Bcl2:Spic*^{tet} abl pre-B cells treated with imatinib for 48 h in the absence (−) or presence (+) of 2 μM doxycycline (Dox) to induce SPIC expression.

(F) Re-ChIP for BCLAF1 after primary ChIP for SPIC or PU.1 (using anti-HA antibodies) in *Rag1*$^{-/-}$*:Bcl2:Spic*^{tet} or *Rag1*$^{-/-}$*:Bcl2:Pu.1*^{tet} abl pre-B cells, respectively, treated with imatinib and 2 μM doxycycline for 48 h.

(G) ChIP-qPCR of BCLAF1 binding at the *Syk* promoter in *Rag1*$^{-/-}$*:Bcl2* and *Art*$^{-/-}$*:Bcl2* abl pre-B cells treated with imatinib for 48 h.

Data in (A–C) are representative of three independent experiments. Data in (E–G) are mean and SE for three independent experiments. **p ≤ 0.01, ***p ≤ 0.001, and ****p ≤ 0.0001. See also Figure S3 and Table S1.

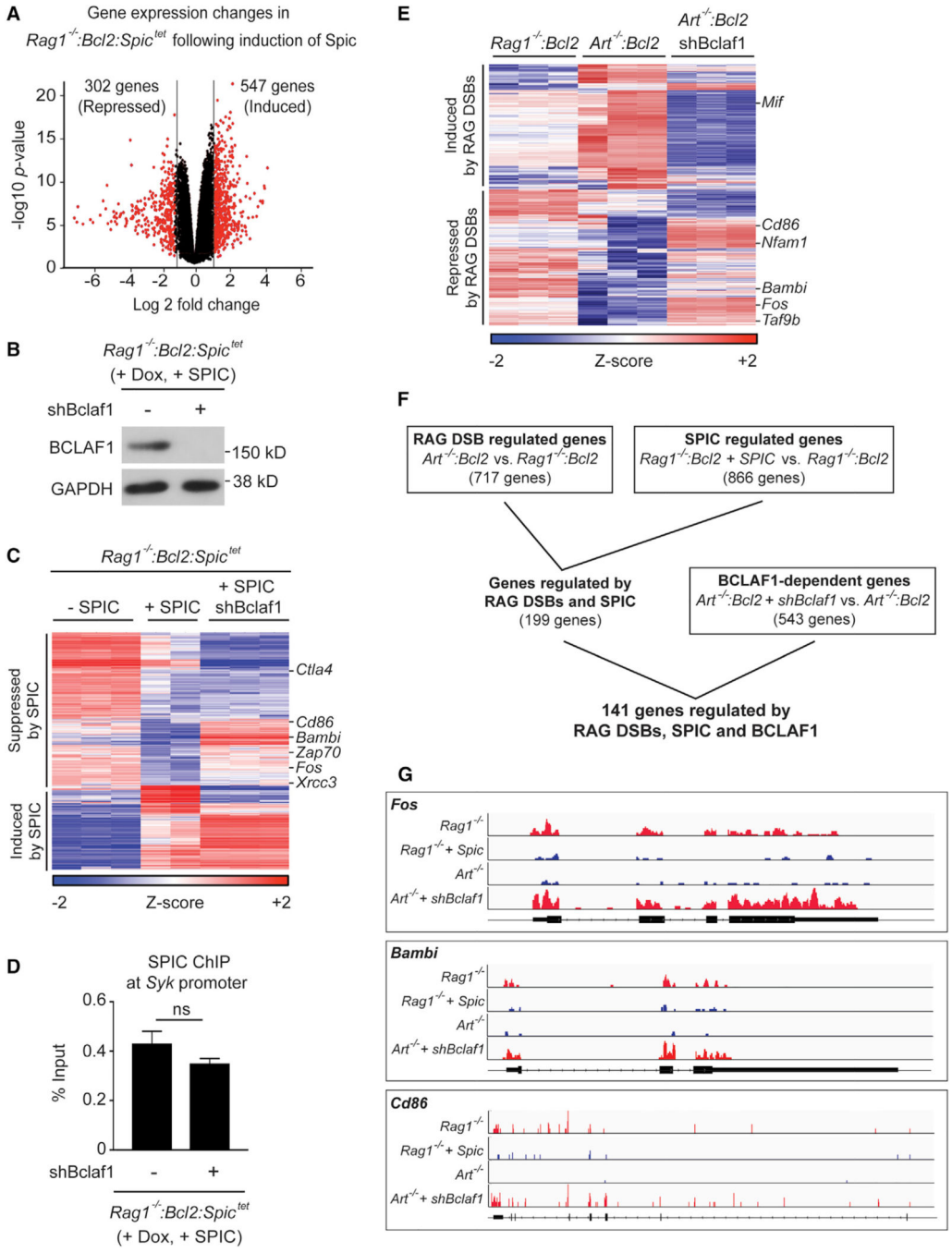

Figure 5. SPIC and BCLAF1 Regulate Gene Expression in Pre-B Cells in Response to RAG DSBs

(A) Volcano plot of gene expression changes (fold change ≥ 2, p ≤ 0.05) between *Rag1*$^{-/-}$*:Bcl2:Spic*^{tet} abl pre-B cells with and without SPIC induction. RNA-seq was performed on *Rag1*$^{-/-}$*:Bcl2:Spic*^{tet} abl pre-B cells treated with imatinib alone (− SPIC) or with imatinib and 2 μM doxycycline (+ SPIC) for 48 h. Data are from two independent cultures for each treatment.

(B) Western blot of BCLAF1 in *Rag1*$^{-/-}$*:Bcl2:Spic*^{tet} abl pre-B cells transduced with a retrovirus expressing a scrambled short hairpin RNA (shRNA) (−) or shBclaf1 (+) and then

treated with imatinib and 2 μM doxycycline for 48 h (to induce SPIC). Data are representative of three independent experiments.

(C) Heatmap of gene expression changes (fold change ≥ 2, $p \leq 0.05$) among *Rag1*$^{-/-}$*:Bcl2:Spic*^{tet} cells without SPIC, *Rag1*$^{-/-}$*:Bcl2:Spic*^{tet} cells expressing SPIC, and *Rag1*$^{-/-}$*:Bcl2:Spic*^{tet} cells expressing SPIC and shBclaf1. Cells were treated as in (A) and (B). Columns represent independent cultures for each cell line and treatment as indicated. Representative gene are delineated to the right.

(D) ChIP-qPCR of SPIC binding at the *Syk* promoter in *Rag1*$^{-/-}$*:Bcl2:Spic*^{tet} cells expressing a scrambled shRNA (−) or shBclaf1 (+) and treated as in (B). Data are mean and SE for three independent experiments. ns, not significant.

(E) Heatmap of gene expression changes (fold change ≥ 2, $p \leq 0.05$) among *Rag1*$^{-/-}$*:Bcl2,* *Art*$^{-/-}$*:Bcl2,* and *Art*$^{-/-}$*:Bcl2* abl pre-B cells expressing shBclaf1. *Art*$^{-/-}$*:Bcl2* abl pre-B cells were transduced with a retrovirus expressing shBclaf1. RNA sequencing (RNA-seq) was performed on all cells after treatment with imatinib for 48 h. Columns represent independent cultures for each cell line as indicated. Representative genes are delineated to the right.

(F) Flow diagram showing identification of genes regulated by RAG DSBs, SPIC, and BCLAF1 in pre-B cells.

(G) Representative tracks at genes identified in F from RNA-seq in (C) and (E).

See also Figures S4 and S5 and Tables S2, S3, and S4.

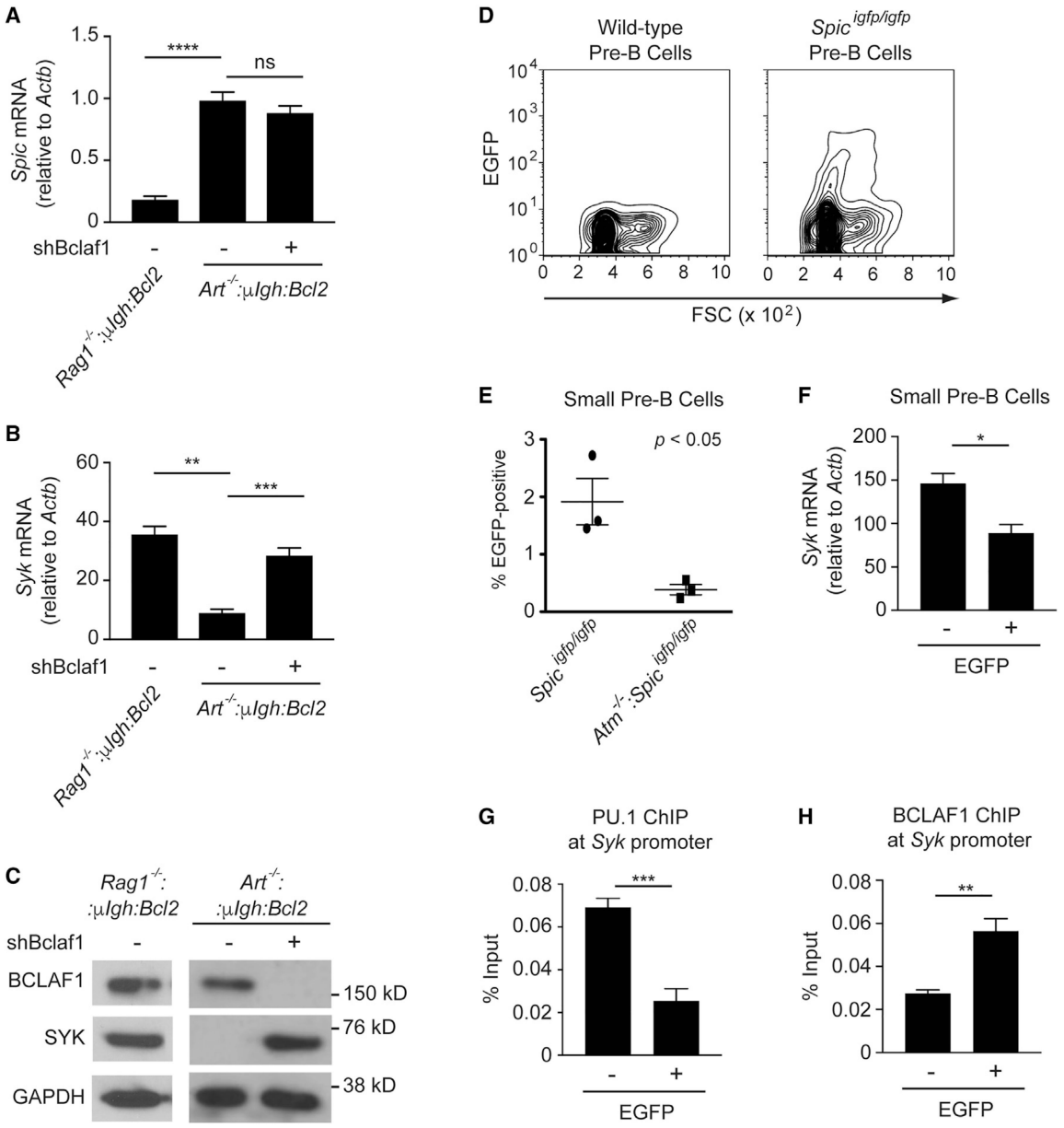

Figure 6. BCLAF1 Regulates SYK Expression in Primary Pre-B Cells

(A-C) *Art*$^{-/-}$*:μIgh:Bcl2* pre-B cells were transduced with a retrovirus expressing a scrambled shRNA (−) or shBclaf1 (+) and then subsequently withdrawn from IL-7.

(A and B) *Spic* and *Syk* mRNA expression assessed in indicated small pre-B cells 2 days after IL-7 withdrawal. Data are mean and SE for three independent experiments.

(C) Western blot of SYK and BCLAF1 in indicated small pre-B cells 2 days after IL-7 withdrawal. Data are representative of three independent experiments.

(D) Flow cytometric analysis showing EGFP (y axis) and FSC (x axis) in bone marrow pre-B cells (B220^{lo}CD43^{-}IgM^{-}) from wild-type and *Spic*$^{igfp/igfp}$ mice. Data are representative of five independent experiments.

(E) Percentage of EGFP-positive small pre-B cells in *Spic*$^{igfp/igfp}$ (circles) and *Atm*$^{-/-}$*:Spic*$^{igfp/igfp}$ (squares) mice was quantified by flow cytometry as in (D). Data are mean and SE from three independent mice of each genotype.

(F–H) *Syk* mRNA expression (F), ChIP-PCR of PU.1 at *Syk* promoter (G), and ChIP-PCR of BCLAF1 at *Syk* promoter (H) in EGFP-negative (−) and EGFP-expressing (+) small pre-B cells sorted from *Spic*$^{igfp/igfp}$ mice. Data in (F) are the mean and SE from three independent experiments. Data in (G) and (H) are representative of two independent experiments.

*p ≤ 0.05, **p ≤ 0.01, ***p ≤ 0.001,****p ≤ 0.0001; ns, not significant.

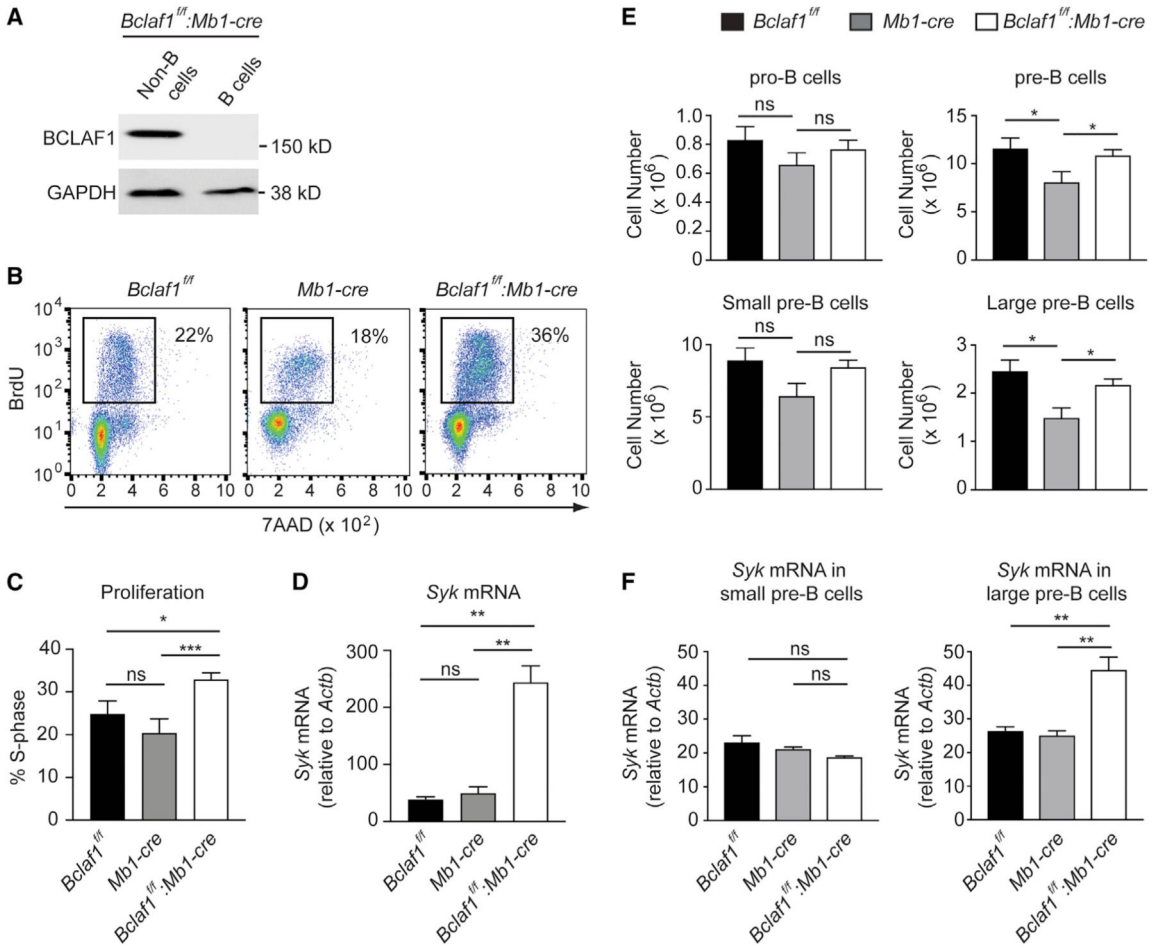

Figure 7. BCLAF1 Regulates Large to Small Pre-B Cell Transition

(A) Western blot of BCLAF1 in sorted CD19− (non-B cell) and CD19+ B cell populations from bone marrow of 5-week-old *Bclaf1*$^{f/f}$*:Mb1-cre* mice. Data are representative of three independent mice.

(B) Flow cytometric analysis of BrdU incorporation (y axis) and DNA content (7AAD, x axis) performed 24 h after IL-7 withdrawal. Percentage of cells that entered S phase during BrdU labeling (box) is indicated. Data are representative of at least three independent experiments.

(C) Percentage of cells that entered S phase in cell cycle analysis performed in (B). Data are mean and SE for four independent experiments.

(D) *Syk* mRNA expression 24 h after IL-7 withdrawal. Data are mean and SE for three independent experiments.

(E) Quantitation of flow cytometric analysis of pro-B cells ($B220^{lo}IgM^{-}CD43^{+}$) and pre-B cells ($B220^{lo}IgM^{-}CD43^{-}$) in bone marrow of 5-week-old *Bclaf1*$^{f/f}$ (black bars, n = 12), *Mb1-cre* (gray bars, n = 9), and *Bclaf1*$^{f/f}$*:Mb1-cre* (white bars, n = 12) mice. Large and small pre-B cells were gated on the basis of forward-scatter and side-scatter characteristics.

(F) *Syk* mRNA expression in small and large pre-B cells sorted from 5-week-old *Bclaf1*$^{f/f}$ (black bars, n = 4), *Mb1-cre* (gray bars, n = 5), and *Bclaf1*$^{f/f}$*:Mb1-cre* (white bars, n = 5) mice.

Data in (E) and (F) are mean and SE for indicated numbers of mice. *p ≤ 0.05, **p ≤ 0.01, and ***p ≤ 0.001; ns, not significant.

See also Figure S6.

KEY RESOURCES TABLE

REAGENT or RESOURCE	SOURCE	IDENTIFIER
Antibodies		
APC human CD25 Clone BC96	BioLegend	Cat# 302610; RRID: AB_314280
biotin conjugated anti-hCD2	BD Biosciences	Cat# 555325; RRID: AB_395732
PE- anti-hCD25 Clone BC96	BioLegend	Cat# 302605; RRID: AB_314275
FITC-conjugated anti-CD45R/B220 (clone RA3–6B2)	BD Biosciences	Cat# 553088; RRID: AB_394618
PE-conjugated anti-CD43 (clone S7)	BD Biosciences	Cat# 553271: RRID: AB_394748
FITC-conjugated anti-CD43 (clone S7)	BD Biosciences	Cat# 553270; RRID: AB_394747
PE-Cy7-conjugated anti-CD45/B220 (clone RA3–6B2)	BD Biosciences	Cat # 552772: RRID: AB_394458
allophycocyanin (APC)-conjugated anti-IgM (clone II/41)	BD Biosciences	Cat # 550676; RRID: AB_398464
PE-conjugated anti-hCD2	BD Biosciences	Cat# 555327; RRID: AB_395734
APC-conjugated anti-hCD2	BD Biosciences	Cat# 560642; RRID: AB_1727443
Anti-SYK (clone D1I5Q)	Cell Signaling Technology	Cat# 12358; RRID: AB_2687923
Anti-BCLAF1 antibody (A300–608A)	Bethyl Laboratories	Cat# A300–608A; RRID: AB_513581
PU.1 (PA5–17505)	Thermo Fisher	Cat# 17505; RRID: AB_?0989141
Anti-GAPDH	Cell Signaling	Cat# 5174; RRID: AB_10622025
anti-FLAG (clone M2)	Sigma	Cat# 1804; RRID: AB_262044
HRP-conjugated anti-mouse IgG	Cell Signaling	Cat # 7074; RRID: AB_2099233
HRP-conjugated anti-rabbit IgG	Cell Signaling	Cat# 7065; RRID: AB_10890862
Anti-HA	Abcam	Cat# ab9110; RRID: AB_307019
control rabbit IgG	Millipore	Cat# 06–371; RRID: AB_390146
Chemicals, Peptides, and Recombinant Proteins		
SuperScriptII	Life Technologies	18064–014
Brilliant II SYBR Green	Agilent	600828
Interleukin-7 (IL-7)	Miltenyi Biotec	130–098–222
Imatinib	Novartis	00078–0438–15
Lipofectamine 2000	Life Technologies	11668–019
PEG-8000	Fisher	P156–500
Sequabrene	Sigma	S 2667
ATM inhibitor KU55933	Tocris	3544
Micrococcal nuclease	New England Biolabs	M0247S
Critical Commercial Assays		
RNeasy	QIAGEN	74104
Protein A Dynabeads	Thermo Fisher Scientific	10002D
QIAquick PCR purification kit	QIAGEN	28106
Anti-biotin magnetic beads	Miltenyi Biotec	130–090–485
Anti-hCD25 magnetic beads	Miltenyi Biotec	130–092–983
Anti-hCD2 magnetic beads	Miltenyi Biotec	130–091–114

REAGENT or RESOURCE	SOURCE	IDENTIFIER
High sensitivity DNA ChiPs	Agilent Technologies	5067–4626
Magnetic Separation columns	Miltenyi Biotec	130–042–201
ECL	Pierce	32209
ECL Prime	GE Healthcare	RPN2232
FITC BrdU Flow Kit	BD Bioscience	559619
Deposited Data		
ChiP-seq	This paper	NCBI GEO #: GSE129130 (subseries: GSE129124)
RNA-seq	This paper	NCBI GEO #: GSE129130 (subseries: GSE129129)
Experimental Models: Cell Lines		
Art$^{-/-}$*:Bcl2* abl pre-B cell	Barry Sleckman	N/A
Rag$^{-/-}$*:Bcl2* abl pre-B cell	Barry Sleckman	N/A
PlatE	Cell Biolabs, Inc	RV-101
Experimental Models: Organisms/Strains		
Mb1-cre (Cd79a$^{tm1(cre)Reth}$) mice	Jackson Laboratory	20505
Bclaf1$^{f/f}$ mice	KOMP Repository	*Bclaf1*^{tm1a}
Rag1$^{-/-}$*:μIgh:Bcl2*	Barry Sleckman	N/A
Art$^{-/-}$*:μIgh:Bcl2*	Barry Sleckman	N/A
B6.Cg-Tg(ACTFLPe)9205Dym/J	Jackson Laboratory	5703
Spic$^{igfp/igfp}$	Kenneth Murphy	N/A
Oligonucleotides		
Primers are listed in Table S5	This paper	N/A
Recombinant DNA		
MSCV-hCD2-mir30 vector	Mark Schlissel	N/A
pFLRU-TRE-FLAG-HA-PU.1-Ubc-rtTA-IRES-Thy1.2	This paper	N/A
pFLRU-TRE-FLAG-HA-SPIC-Ubc-rtTA-IRES-Thy1.2	This paper	N/A
pCMV-VSV-G	Stewart et al., 2003	Addgene #8454
pCMV-d8.2R dvpr	Stewart et al., 2003	Addgene #8455
Software and Algorithms		
Bowtie v. 1.1.2	Langmead and Salzberg, 2012	http://bowtie-bio.sourceforge.net/bowtie2/index.shtml RRID:SCR_005476
MACS version 2	Zhang et al., 2008	http://liulab.dfci.harvard.edu/MACS/ RRID:SCR_013291
Galaxy V18.09	Afgan et al., 2016	https://usegalaxy.org RRID:SCR_006281
GenomicRanges	Lawrence et al., 2013	https://www.bioconductor.org/packages//2.10/bioc/html/GenomicRanges.html RRID:SCR_000025
Bedtools V2.25.0	Quinlan and Hall, 2010	https://github.com/arq5x/bedtools2. RRID:SCR_006646
EdgeR- TMM	Robinson et al., 2010	http://bioconductor.org/biocLite.R RRID:SCR_012802
Limma-Voom	Law et al., 2014	https://omictools.com/limma-tool RRID:SCR_010943

REAGENT or RESOURCE	SOURCE	IDENTIFIER
TreeView Version 1.1.6r4	Saldanha, 2004	https://bitbucket.org/TreeView3Dev/treeview3/ RRID:SCR_016916
Heatmap3	Zhao et al., 2014	https://bioconductor.org/packages/release/bioc/html/heatmaps.html
DAVID (v.6.8)	Huang et al., 2009	https://david.ncifcrf.gov RRID:SCR_001881
EaSeq (v1.111)	Lerdrup et al., 2016	http://easeq.net
MAnorm	Shao et al., 2012	http://bcb.dfci.harvard.edu/~gcyuan/MAnorm/MAnorm.htm RRID:SCR_010869
Prism 8 (v8.0.2)	GraphPad Software	https://www.graphpad.com